https://doi.org/10.1093/plphys/kiac550 PLANT PHYSIOLOGY 2023: 191: 1884–1912

Plant Physiology®

Research Article

A superior gene allele involved in abscisic acid signaling enhances drought tolerance and yield in chickpea

Virevol Thakro [1], Naveen Malik [1,2], Udita Basu [1], Rishi Srivastava [1], Laxmi Narnoliya [1], Anurag Daware [1], Nidhi Varshney [1], Jitendra K. Mohanty [1], Deepak Bajaj [1], Vikas Dwivedi [1], Shailesh Tripathi [3], Uday Chand Jha [4], Girish Prasad Dixit [4], Ashok K. Singh,[3] Akhilesh K. Tyagi [1,5], Hari D. Upadhyaya [6,*] and Swarup K. Parida [1,*]

1 Genomics-assisted Breeding and Crop Improvement Laboratory, National Institute of Plant Genome Research (NIPGR), Aruna Asaf Ali Marg, New Delhi 110067, India
2 Amity Institute of Biotechnology, Amity University Rajasthan, Jaipur 303002, India
3 Division of Genetics, Indian Agricultural Research Institute (IARI), New Delhi 110012, India
4 Crop Improvement Division, Indian Institute of Pulses Research (IIPR), Kanpur 208024, India
5 Department of Plant Molecular Biology, University of Delhi, South Campus, New Delhi 110021, India
6 Genebank, International Crops Research Institute for the Semi-Arid Tropics (ICRISAT), Patancheru 502324, Telangana, India

*Author for correspondence: swarup@nipgr.ac.in (S.K.P.), harideo.upadhyaya@gmail.com (H.D.U.)

V.T., N.M., U.B., L.N., N.V., J.K.M., D.B., and V.D. performed the field and laboratory experiments and drafted the manuscript. H.D.U., S.T., U.C.J., and G.P.D. helped construct the association panel and mapping population and performed field phenotyping. V.T., R.S., and A.D. conducted the genotyping and all genome data analyses. A.K.S., A.K.T., H.D.U., and S.K.P. conceived and designed the study, guided data analysis and interpretation, and participated in drafting and revising the manuscript. All authors gave final approval of the version to be published.
The author responsible for distribution of materials integral to the findings presented in this article in accordance with the policy described in the Instructions for Authors (https://academic.oup.com/plphys/pages/General-Instructions) is: Swarup K. Parida (swarup@nipgr.ac.in).

Abstract

Identifying potential molecular tags for drought tolerance is essential for achieving higher crop productivity under drought stress. We employed an integrated genomics-assisted breeding and functional genomics strategy involving association mapping, fine mapping, map-based cloning, molecular haplotyping and transcript profiling in the introgression lines (ILs)- and near isogenic lines (NILs)-based association panel and mapping population of chickpea (*Cicer arietinum*). This combinatorial approach delineated a bHLH (basic helix–loop–helix) transcription factor, *CabHLH10* (*Cicer arietinum bHLH10*) underlying a major QTL, along with its derived natural alleles/haplotypes governing yield traits under drought stress in chickpea. CabHLH10 binds to a *cis*-regulatory G-box promoter element to modulate the expression of *RD22* (responsive to desiccation 22), a drought/abscisic acid (ABA)-responsive gene (via a *trans*-expression QTL), and two strong yield-enhancement photosynthetic efficiency (PE) genes. This, in turn, upregulates other downstream drought-responsive and ABA signaling genes, as well as yield-enhancing PE genes, thus increasing plant adaptation to drought with reduced yield penalty. We showed that a superior allele of *CabHLH10* introgressed into the NILs improved root and shoot biomass and PE, thereby enhancing yield and productivity during drought without compromising agronomic performance. Furthermore, overexpression of *CabHLH10* in chickpea and Arabidopsis (*Arabidopsis thaliana*) conferred enhanced drought tolerance by improving root and shoot agro-morphological traits. These findings facilitate translational genomics for crop improvement and the development of genetically tailored, climate-resilient, high-yielding chickpea cultivars.

Received May 24, 2022. Accepted October 15, 2022. Advance access publication December 7, 2022

Open Access

Introduction

The major staple food cereal and legume crops are severely affected by drought, which causes substantial yield and productivity losses world-wide (Fang et al., 2010; Varshney et al., 2018a, b). Chickpea (*Cicer arietinum* L.) is an economically important major grain legume crop cultivated by the resource-poor farmers in the arid and the semi-arid regions across the globe (Varshney et al., 2013a). Since approximately 90% of the world's chickpea is widely cultivated on residual soil moisture in rainfed environments, its productivity is adversely affected by terminal drought stress resulting in substantial (more than 50%) annual yield losses (Varshney et al., 2018a, b). It is, therefore, crucial to develop high-yielding, climate-ready chickpea varieties that can sustain drought stress to ensure global food security.

Terminal drought is a type of soil moisture stress where the crop grows and matures on gradually depleting soil moisture with increasing severity at the time of maturity towards end of the growing season (Gaur et al., 2015). It predominantly affects diverse agro-morphological, physiological and yield component traits including anthesis, pollen viability/fertilization, pollen tube growth, stigma/style function, fertility, pod filling, pod size, seed growth/development, and photosynthetic efficiency (PE) leading to low pod/seed number, reduced biomass and harvest index, consequently resulting in low seed yield and productivity in chickpea (Fang et al., 2010; Mir et al., 2012; Hamwieh et al., 2013; Krishnamurthy et al., 2013; Nakashima et al., 2014; Pang et al., 2017).

Plants have evolved wide arrays of adaptive mechanisms including morphological, physiological, biochemical, cellular, and molecular responses to cope up with drought stress (Abe et al., 2003). The phytohormone abscisic acid (ABA) plays a major role in regulating the response and tolerance against drought stress by inducing the expression of a diverse array of downstream drought- and ABA-responsive genes (Abe et al., 2003). Drought triggers plants to accumulate ABA through induction of ABA biosynthetic genes leading to various agro-morphological and physiological changes such as stomatal closure, reduced leaf size, water-use efficiency, inhibition of shoot growth, lateral root formation, and root elongation (Abe et al., 2003; Umezawa et al., 2010). Certain key mechanisms involve ABA-mediated stomatal closure to reduce transpiration and minimize water loss and/or enhance root cell elongation so as to maximize water uptake during drought stress (Tuteja, 2007; Muhammad Aslam et al., 2022).

Despite numerous reports on the role of ABA in plant drought tolerance, its effect on crop yield performance during drought is unexpectedly meagre and thus far from comprehensive (Bao et al., 2016). Several studies, however, suggest that ABA improves biomass and grain yield under moderate drought conditions in wheat (*Triticum aestivum*; Travaglia et al., 2007, 2010), soybean (*Glycine max*; Travaglia et al., 2009), rice (*Oryza sativa*; Yang et al., 2001, 2004) and rapeseed (*Brassica napus*; Wang et al., 2005) by enhancing carbon allocation, transportation and their active partitioning in seeds. Since ABA has a positive effect on grain filling during drought, optimizing the physiological processes in response to ABA signalling has the potential to improve drought tolerance without compromising yield. Improving drought tolerance without compromising yield and productivity in water-limited environments is a major challenge in crop improvement program (Venuprasad et al., 2007). Identifying key traits that maximizes crop yield and productivity under drought stress is therefore critical to develop high-yielding, drought-tolerant crops (Varshney et al., 2018a). Various key physiological traits contributing to yield under drought stress include early maturity, leaf water potential, relative water content, water-use efficiency, transpiration efficiency, carbon isotope discrimination ($\Delta^{13}C$), crop growth and partitioning rate, root traits, shoot biomass, and PE (Upadhyaya et al., 2012; Kashiwagi et al., 2013, 2015; Krishnamurthy et al., 2013; Ramamoorthy et al., 2016; Basu et al., 2019). Considerable progress has been made in improving drought tolerance and yield through direct selection for major yield traits including pod number, seed number, seed weight, and yield per plant during drought stress in several crops such as rice (Guan et al., 2010; Venuprasad et al., 2007, 2008; Raman et al., 2012), wheat (Sivamani et al., 2000; Guóth et al., 2009), and chickpea (Talebi and Karami, 2011; Upadhyaya et al., 2012; Varshney et al., 2014a). Similarly, modification of root system architecture is another vital trait for improving crop grain yield due to its ability to efficiently absorb water from deeper soils in water-limited environments (Kashiwagi et al., 2015; Prince et al., 2017). Therefore, direct selection of seed yield in conjunction with various yield component traits under drought stress appears to be the most promising strategy for selecting stable, durable, and high-yielding crop genotypes in drought-prone environments (Kashiwagi et al., 2015; Prince et al., 2017).

Deciphering the genetic and molecular mechanism governing complex drought-tolerance traits is essential for genomics-assisted crop improvement in order to develop high-yielding, drought-tolerant crops varieties. Traits contributing to drought tolerance are generally complex quantitative with multifaceted nature, low heritability and also influenced by large genotype-by-environment ($G \times E$) interactions (Varshney et al., 2014a; Kashiwagi et al., 2015). Transcription factors (TFs) like MYC (myelocytomatosis), MYB (myeloblastosis), NAC [NAM (no apical meristem), ATAF (Arabidopsis transcription activator factor), and CUC (cup-shaped cotyledon)], ABF [ABRE (ABA-responsive element)-binding factors)], ABI (ABA-insensitive), bZIP (basic leucine zipper), and dehydration-responsive element-binding are the key regulators that play the vital role in drought response by modulating the expression of a diverse array of specific downstream genes via either ABA-dependent and ABA-independent signaling pathways (Singh and Laxmi, 2015; Sah et al., 2016). Numerous other genes involved in these pathways essentially encode diverse sets of biosynthetic enzymes [*ZEP* (zeaxanthin epoxidase), *AAO3* (ABA-aldehyde oxidase 3), *NCED3* (9-cis-epoxycarotenoid dioxygenase 3), *ABA3*

(ABA-deficient 3)], receptors [PYR (pyracbactin resistance), PYL (pyracbactin resistance-like), ABP9 (ABRE binding protein 9), OST1 (open stomata1)] as well as ABRE and DRE *cis*-elements binding factors (Singh and Laxmi, 2015; Dar et al., 2017). Substantial efforts have been made in the genetic and molecular dissection of various complex drought-tolerance quantitative traits that contribute to higher yield in a variety of crop species including rice, wheat, and soybean (Maccaferri et al., 2008; Li et al., 2013; Uga et al., 2013; Selvaraj et al., 2017; Mao et al., 2022; Zhao et al., 2022) as well as the model plant Arabidopsis (*Arabidopsis thaliana*) (Abe et al., 2003; Ramírez et al., 2009; Roca et al., 2019). Unfortunately, no such comprehensive efforts so far on understanding the complex genetic architecture of drought-tolerance traits contributing to higher yield and productivity are being made in chickpea. No single robust gene and allele has been identified yet to confer drought tolerance and enhance chickpea crop yield and productivity in multiple genetic backgrounds/environments without associated epistatic/pleiotropic effects on other desirable agro-morphological traits. This lack of functionally relevant drought-tolerance gene and natural allele impedes efforts for marker-assisted genetic improvement and development of drought-tolerant, high-yielding cultivars of chickpea.

In this study, we employed a combined genomics-assisted breeding and functional genomics strategy to decipher the genetic and molecular architecture of complex drought-tolerance quantitative traits in chickpea. Using a phenotypically well-characterized near-about homogeneous introgression lines (ILs)- and near isogeneic lines (NILs)-based association panel and mapping population, we successfully delineated *CabHLH10*, a promising transcription factor (TF) gene of a major quantitative trait locus (QTL) and its derived natural alleles governing yield/productivity traits under drought stress in chickpea. *CabHLH10* confers drought tolerance as well as enhances yield and productivity during drought stress by modulating the transcriptional regulation of its targets including *RD22*, a drought-responsive gene and two yield-enhancing PE genes in response to ABA signaling. We showed that CabHLH10 binds to *cis*-regulatory G-box promoter elements of *RD22* and PE genes via a *trans*-expression QTL (*trans*-eQTL). This effect in turn upregulates other downstream drought-responsive ABA signaling as well as PE genes, thereby enhancing drought tolerance with increased yield and productivity. We successfully introgressed a superior natural allele of *CabHLH10* via marker (haplotype)-assisted selection to develop a drought-tolerant chickpea cultivar with enhanced yield and productivity without compromising its agronomic performance.

Results

GWAS and regional association analysis scan potential genomic loci associated with yield traits under drought stress in chickpea

To identify genomic loci associated with yield/productivity traits under drought stress in chickpea, an association panel comprising 222 near-about homogeneous ILs was constituted for GWAS (Supplemental Figures 1 and 2; Supplemental Table 1). For large-scale discovery and high-throughput genotyping of SNPs at a genome-wide scale, whole-genome resequencing of these 222 ILs along with seven *desi*, *kabuli* and wild chickpea accessions (used as parents to develop ILs) was performed. This produced a total of ~336.5 Gb sequence data with an average sequencing depth of ~2.0X (1.6 Gb) per IL/accession, demonstrating 87.5% coverage of the reference chickpea genome (Supplemental Table 2). This altogether discovered ~2.3 million high-quality SNPs of which 110110 SNPs were genotyped in all 222 ILs belonging to an association panel (Supplemental Table 3). The identified SNPs were structurally and functionally annotated on the diverse coding, and non-coding intronic and upstream/downstream regulatory (URR/DRR) sequence components of 16114 genes (44933 SNPs) as well as intergenic regions (65177 SNPs) representing eight chromosomes and unanchored scaffolds of chickpea genome (Supplemental Figure 3, Supplemental Figure 4, A–D).

The use of 48167 chromosome-wise SNPs with high minor allele frequency (MAF $\geq$ 0.13) in the phylogenetic tree construction, population structure and principal component analysis (PCA) clustered the association panel of 222 ILs into a single population group (POP I) and exhibited very low population genetic structure (0.061 mean Fst) (Figure 1, A–B; Supplemental Figure 5, A–D). The association panel representing POP I exhibited significant linkage disequilibrium (LD) decay at a physical distance of 100 kb across the chromosomes (Figure 1C). The large-scale multi-environment field phenotyping of 222 ILs belonging to an association panel exhibited wide phenotypic variation and high heritability for seven yield traits under irrigated (unstressed) versus unirrigated (drought stress) conditions including drought yield index per plant/hectare [DYI(P/H)] across three individual and over all years (Supplemental Figures 6 and 7; Supplemental Table 4).

GWAS analysis was performed by integrating the yield traits phenotyping data during unstressed irrigated and drought stress unirrigated conditions with genome-wide genotyping information of 48167 chromosome-wise SNPs and genetic relatedness (single population with very low population genetic structure) data among 222 ILs of an association panel. This analysis detected 14 genomic loci in 12 genes mapped on five chromosomes showing significant association with the yield traits in at least across two of the three environments under both unstressed and drought stress conditions including DYI(P/H) (Figure 1, D–E; Supplemental Figures 8 and 9; Supplemental Table 5). The phenotypic variation explained (PVE) by the 14 associated genomic loci for DYI(P/H) traits varied from 10.0% to 28.7% (10^{-8} to 10^{-9} P) (Supplemental Table 5). Among 14 loci, two informative SNPs [Ca1:12709839(T/A) and Ca1:12709928(G/T)] in the URR of a *bHLH* (basic helix–loop–helix) TF gene, mapped on chromosome 1, exhibited strong association (27.6%–28.7% PVE, 10^{-9} P) with DYI(P/H) across all three environments (Figure 1, D–E; Supplemental Table 5). The use of

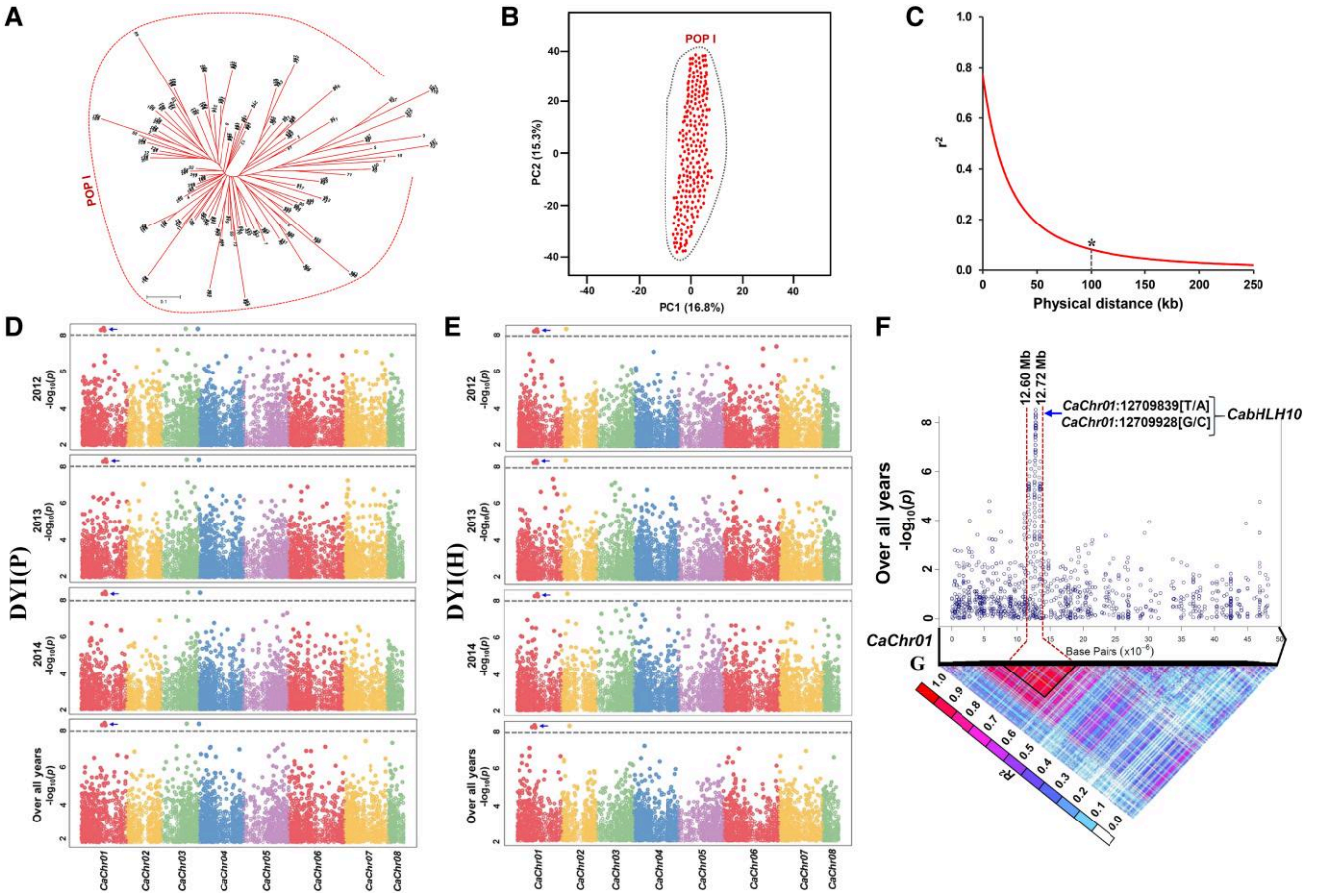

Figure 1 High-resolution association mapping identified potential genomic loci showing strong association with DYI in chickpea. Determination of molecular diversity, phylogenetic relationship, and historical recombination (LD) among 222 introgression lines (ILs) in an association panel based on (A) unrooted phylogenetic tree construction, (B) PCA and (C) LD decay (mean r^2) estimation using 48167 SNPs mapped across eight chromosomes. Digits mentioned in the clades of phylogenetic tree correspond to IL numbers given in the Supplemental Table 1. The scale bar (scale: 0.1) below the phylogenetic tree refers to the evolutionary distances computed based on units of the number of nucleotide substitutions per site. B, In PCA, clustering of all 222 ILs into a single population group (POP I) in which the PC1 and PC2 explained 16.8% and 15.3% of the total variance, respectively. C, In the LD decay, the plotted curved lines representing a population (POP I) signify the mean r^2 values among SNPs spaced with uniform 50 kb physical intervals from 0 to 250 kb across chromosomes. The dotted line represents the significant LD decay in a population of constituted chickpea association panel. *Significant difference of mean r^2 value at a 100 kb chromosomal physical position as compared to that estimated at 0, 50, 150, and 250 kb ($P < 0.001$, Student's *t*-test). D and E, GWAS-derived Manhattan plots generated using 48167 chromosome-wise SNPs showing the significant *P* values of genomic SNP loci associated with drought yield index per plant [DYI(P)] (D) and drought yield index per hectare [DYI(H)] (E) across years. The SNP genotyping and DYI(P/H) trait phenotyping information evaluated among 222 ILs were analyzed under both irrigated (unstressed) and unirrigated (drought stress) conditions by three individual years (2012, 2013, and 2014) and using the overall mean across three years (over all years) to generate the Manhattan plots. The genomic distribution of SNPs mapped on eight chromosomes is indicated on the *x*-axis. The *y*-axis shows the $-log_{10}(P)$ values for SNP loci associated with DYI(P/H) trait. The SNPs exhibiting significant association with DYI(P/H) at a cutoff *P* value $\leq 10^{-8}$ are indicated by dotted lines. F, Gene-by-gene regional association analysis-derived local Manhattan plot and (G) high-resolution LD heat map covering a 120-kb genomic interval (12.60–12.72 Mb with 15 genes) (highlighted with red dotted lines) surrounding the strong [DYI(P/H)]-associated SNP loci [Ca01:12709839(T/A) and Ca01:12709928(G/C)] in the upstream regulatory region (URR) of a *CabHLH10* mapped on chromosome 1. Arrows indicate the genomic positions of DYI(P/H)-associated SNPs identified across three years (over all years) on chromosome 1. In the LD heat map, R^2 indicates the frequency correlation among pair of alleles across a pair of SNP loci. *CaChr01-08* denote *Cicer arietinum* chromosomes 01-08. DYI(P/H): drought yield index per plant/hectare.

chromosome-wise 48167 SNPs much higher (six times) than the required minimal SNP-density of 7400 SNPs to cover the significant LD (100 kb LD decay) in a chickpea genome for GWAS indicates robustness of high-resolution trait association mapping information generated in the present investigation. Therefore, the trait-associated genomic loci uncovered by GWAS have functional relevance for understanding the complex genetic architecture of quantitative yield traits during drought stress in chickpea.

Gene-by-gene regional association analysis was performed to validate the association potential of GWAS-derived genomic loci for yield traits under drought stress in chickpea.

For this, 100 kb genomic region (exhibiting significant LD decay) flanking the trait-associated URR-SNPs in a *bHLH* gene was selected for high-coverage targeted sequencing to discover the high-quality SNPs. The SNP genotyping data was further correlated with multi-environment DYI(P/H) trait phenotyping information of an association panel (222 ILs) for regional association study. This delimited a shortest 120 kb genomic interval (12.60–12.72 Mb with 15 genes) of significant LD resolution (0.87 mean R^2) covering the either side of GWAS-derived URR-SNPs in a *bHLH* which is strongly associated with DYI(P/H) (Figure 1, F–G). Within this LD-block, comprehensive gene-by-gene regional association analysis targeting 15 annotated genes exhibited strong association (34.7% PVE, 10^{-11} P) of these regulatory SNPs in a *bHLH* with DYI(P/H) in chickpea.

Fine-mapping and map-based cloning delineate a *CabHLH10* TF gene of a major QTL governing yield traits under drought stress in chickpea

To validate the involvement of GWAS trait-associated genomic loci (*bHLH*) in conferring drought tolerance to chickpea, molecular mapping of the major drought-responsive QTL and its subsequent fine-mapping/map-based cloning were performed. For high-resolution QTL mapping, a high-density genetic linkage map was constructed using an RIL population [LDYI(P/H)-IL-77 × HDYI(P/H)-IL-105] by assigning 7092 SNPs on eight chromosomes with an average map-density of 0.157 cM (Supplemental Figure 10; Supplemental Table 6). The genome-wide genotyping data of SNPs mapped on a high-density genetic linkage map was further integrated with multi-environment DYI(P/H) field phenotyping information for 190 mapping individuals of an RIL population. This analysis detected two major genomic regions harboring seven robust (validated across three individual and over all environments) QTLs governing yield traits under drought stress including DYI(P/H) mapped on chromosomes 1 and 4 of chickpea (Figure 2, A–B; Supplemental Figure 10). The phenotypic variation explained (PVE) by the QTLs varied from 21.8% to 41.3% (11.3–17.6 LOD).

The major drought-responsive robust 1.7-cM *CaqDYI(P/H)1.1* QTL genomic interval harboring the *bHLH* on chromosome 1 with the maximum PVE (41.3%) and LOD (17.6), was selected for fine mapping and map-based cloning. The *CaqDYI(P/H)1.1* QTL genomic region from the donor lines with low (L) and high (H) DYI(P/H) were back-crossed six times into the genetic backgrounds of their corresponding recurrent drought-tolerant and -sensitive lines to generate two BC_6F_3 NILs, LDYI(P/H)-$NIL^{CaqDYI(P/H)1.1}$ and HDYI(P/H)-$NIL^{CaqDYI(P/H)1.1}$, respectively, exhibiting approximately 92%–95% recovery of the recurrent parental genome (Figure 2C; Supplemental Figures 11 and 12). Using 380 mapping individuals of an F_2 population developed by intercrossing these contrasting NILs [LDYI(P/H)-$NIL^{CaqDYI(P/H)1.1}$ × HDYI(P/H)-$NIL^{CaqDYI(P/H)1.1}$], 32 recombinants were detected between Ca1:12707104(T/C) (39.0 cM, 12,707,104 bp) and Ca1:12713382(G/C) (39.7 cM, 12,713,382 bp) SNPs at a 6.3-kb *CaqDYI(P/H)1.1* QTL genomic interval (Figure 2, C–D). The 6.3-kb QTL interval was narrowed down to a 4.4-kb genomic region in eight promising recombinant lines of the NILs by comprehensive phenotyping following progeny testing of all 32 recombinants (Figure 2E). Structural and functional annotation of this 4.4-kb *CaqDYI(P/H)1.1* QTL genomic interval using the *kabuli* reference chickpea genome identified only a single *bHLH* TF gene. A comprehensive genome-wide survey of *bHLH* genes annotated from the chickpea genome based on characteristics of their encoded bHLH domains detected 135 *bHLH* genes. Of which, the *bHLH* with an *MYC*-type functional domain delineated in a *CaqDYI(P/H)1.1* major QTL genomic region was encoded as a *CabHLH10* (gene accession ID *Ca_02482*) (Supplemental Figure 13A; Supplemental Table 7). Two URR-SNPs tightly linked to the delineated CabHLH10 (Figure 2E), as indicated by the lack of recombination between these target gene loci, were selected as the potential candidate governing yield under drought stress in chickpea. Summarily, two informative SNPs [Ca1:12709839(T/A) and Ca1:12709928(G/T)] in the URR of a *CabHLH10* tightly linked to a major and robust *CaqDYI(P/H)1.1* QTL modulating drought-tolerance traits that contribute to enhanced yield/productivity in chickpea were delineated based on high-resolution QTL/fine mapping and GWAS as well as gene-by-gene regional association analysis. The genomic constitution and comprehensive phylogenetic analysis of *CabHLH10* gene orthologs annotated from genomes of diverse legumes and *Arabidopsis* inferred the high conservation of bHLH domains encoded by this gene across legumes and *Arabidopsis* (Supplemental Figure 13, B–D; Supplemental Table 8).

Superior haplotype of *CabHLH10* governs enhanced yield under drought stress in chickpea

We performed molecular haplotyping of the entire coding and non-coding regions of a *CabHLH10* (7561-bp) via targeted resequencing in 222 ILs, six parental accessions of the ILs, 86 cultivated *desi*, *kabuli* and 81 wild *Cicer* accessions (Supplemental Tables 1 and 9 and 10). This analysis detected 63 SNPs in *CabHLH10*, including two synonymous coding- and 28 URR-SNPs (Figure 3A). Further, molecular haplotyping of *CabHLH10* showed that all identified 63 SNPs including 28 URR-SNPs were co-inherited together as haplotype-blocks that overall constituted two major haplotypes (HAP A and HAP B) in the ILs/accessions used (Figure 3, A–B). No amino acid change in the coding region was observed between two *CabHLH10* gene haplotypes, HAP A and HAP B. Gene haplotype-based association analysis revealed a significant association of haplotypes with yield traits under irrigated unstressed versus unirrigated drought stress conditions across all three individual and over all environments. Especially, HAP A and HAP B were significantly associated with low [LDYI(P/H)] and high [HDYI(P/H)] DYI, respectively (Figure 3, C–E). A higher frequency of HAP B compared

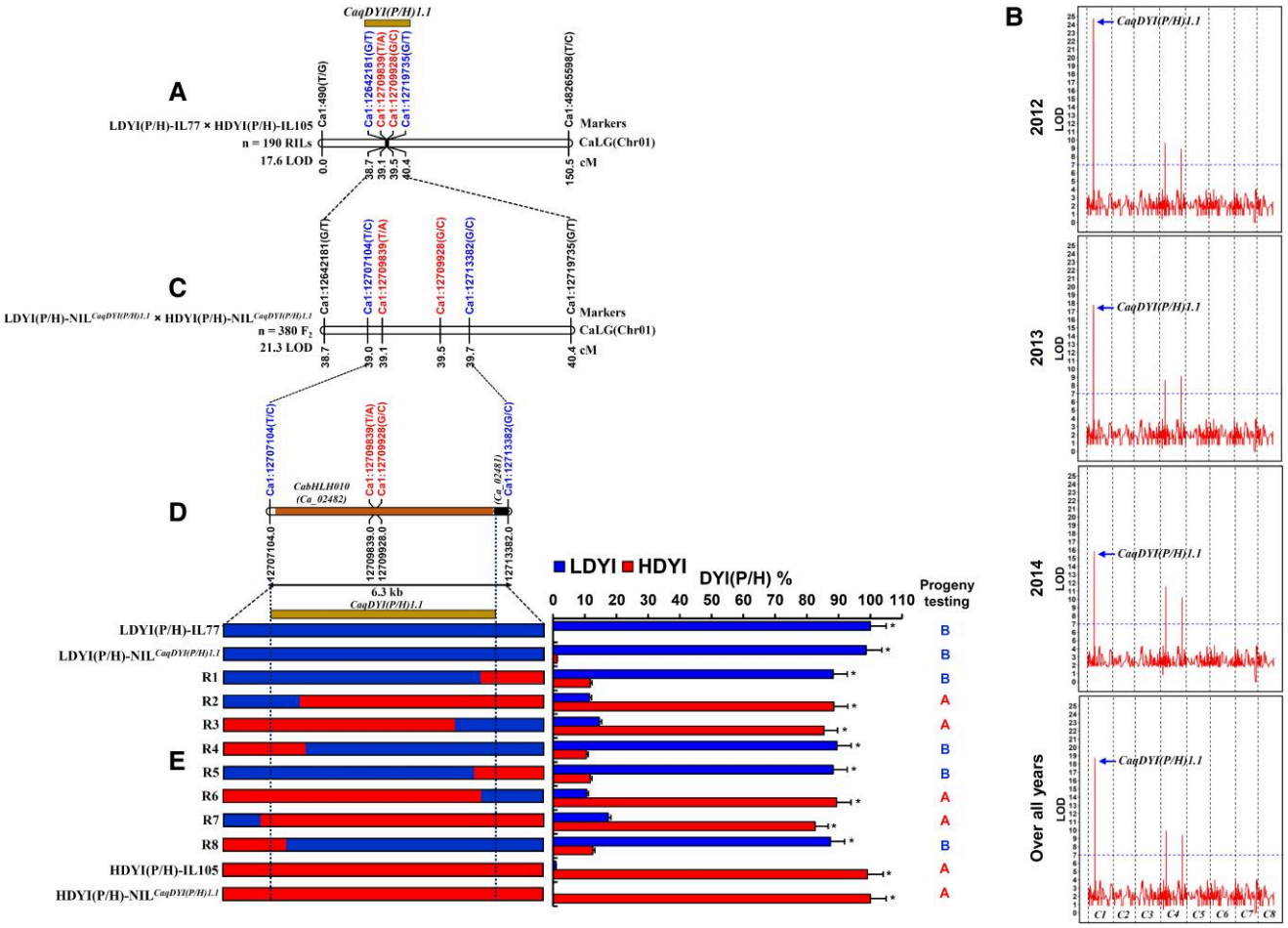

Figure 2 High-resolution molecular mapping and map-based cloning identified a major quantitative trait locus (QTL) genomic region of a *CabHLH10* governing drought tolerance in chickpea. A, Genetic mapping of a major QTL [*CaqDYI(P/H)1.1*] on chromosome 1 of a high-density linkage map using 190 mapping individuals of a RIL population [LDYI(P/H)-IL77 × HDYI(P/H)-IL105]. B, High-resolution QTL mapping depicts the LOD score distribution plots of reaction norms using SNP allele-specific order across years. The dashed line represents the LOD cut-off score of 7.0, permutation $P < 0.001$. Red reaction norm plots indicate [HDYI(P/H)]-specific allele derived from the RIL mapping parental IL [HDYI(P/H)-IL105]. The SNP genotyping and DYI(P/H) trait phenotyping information evaluated among RILs were analyzed under both irrigated (unstressed) and unirrigated (drought stress) conditions by three individual years and using the overall mean across three years (over all years) to generate the reaction norms plots. C1-C8: Chromosomes 1-8 of chickpea. C, Fine-mapping of the *CaqDYI(P/H)1.1* using a mapping population [LDYI(P/H)-*NIL*$^{CaqDYI(P/H)1.1}$ × HDYI(P/H)-*NIL*$^{CaqDYI(P/H)1.1}$] of 380 F_2 individuals with contrasting DYI(P/H) trait. D, The subsequent integration of the genetic and physical map of the fine-mapped target genomic region harboring the *CaqDYI(P/H)1.1* scaled down a 77.5-kb (1.7 cM) QTL interval into a 6.3-kb genomic region with two protein-coding genes including a *bHLH* transcription factor (*CabHLH10*) on chromosome 1. The genetic (cM)/physical (bp) distance and identity of the markers mapped on the LGs/chromosomes are indicated at the lower and upper sides of the chromosomes, respectively. The SNPs flanking and tightly linked with *CaqDYI(P/H)1.1* and *CabHLH10* mapped on chromosome 1, are indicated by blue and red fonts, respectively. E, Progeny testing to deduce the genotype and multi-years replicated field phenotypes of 32 selected recombinants and mapping parental ILs [LDYI(P/H)-IL77 and HDYI(P/H)-IL105] as well as QTL-introgressed NILs [LDYI(P/H)-*NIL*$^{CaqDYI(P/H)1.1}$ and HDYI(P/H)-*NIL*$^{CaqDYI(P/H)1.1}$] for the DYI(P/H) trait. This further narrowed down a 6.3-kb QTL interval into a 4.4-kb genomic region in the eight most promising recombinants of NILs. At this QTL genomic interval, two upstream regulatory region (URR)-derived SNPs [Ca01:12709839(T/A) and Ca01:12709928(G/C)] tightly linked to a *CabHLH10*, demonstrating zero recombination with these target loci in eight selected recombinants of NILs were associated strongly with DYI(P/H) trait. The genomic constitution of high- [HDYI(P/H)] and -low [LDYI(P/H)] DYI(P/H) lines are denoted by "A" and "B," respectively. Horizontal error bars represent mean ± standard deviation ($n = 5$ to 8, independent plants of each IL/NIL), *Significant difference between HDYI(P/H) and LDYI(P/H) at a $P < 0.001$, Student's *t*-test. ILs: Introgression lines. LDYI(P/H) and HDYI(P/H): low and high drought yield index per plant/hectare, respectively. LOD: logarithm of odds.

with HAP A was shared in the parents of ILs (71.5%) followed by wild *Cicer* accessions (69.2%), ILs (61.8%), and cultivated chickpea accessions (53.5%) (Figure 3 B). These findings implicate that the target genomic region (*CabHLH10* gene haplotype/allele) delineated using the wild and cultivated gene pool-derived ILs has a functional relevance to develop drought-tolerant chickpea cultivars with enhanced yield/productivity.

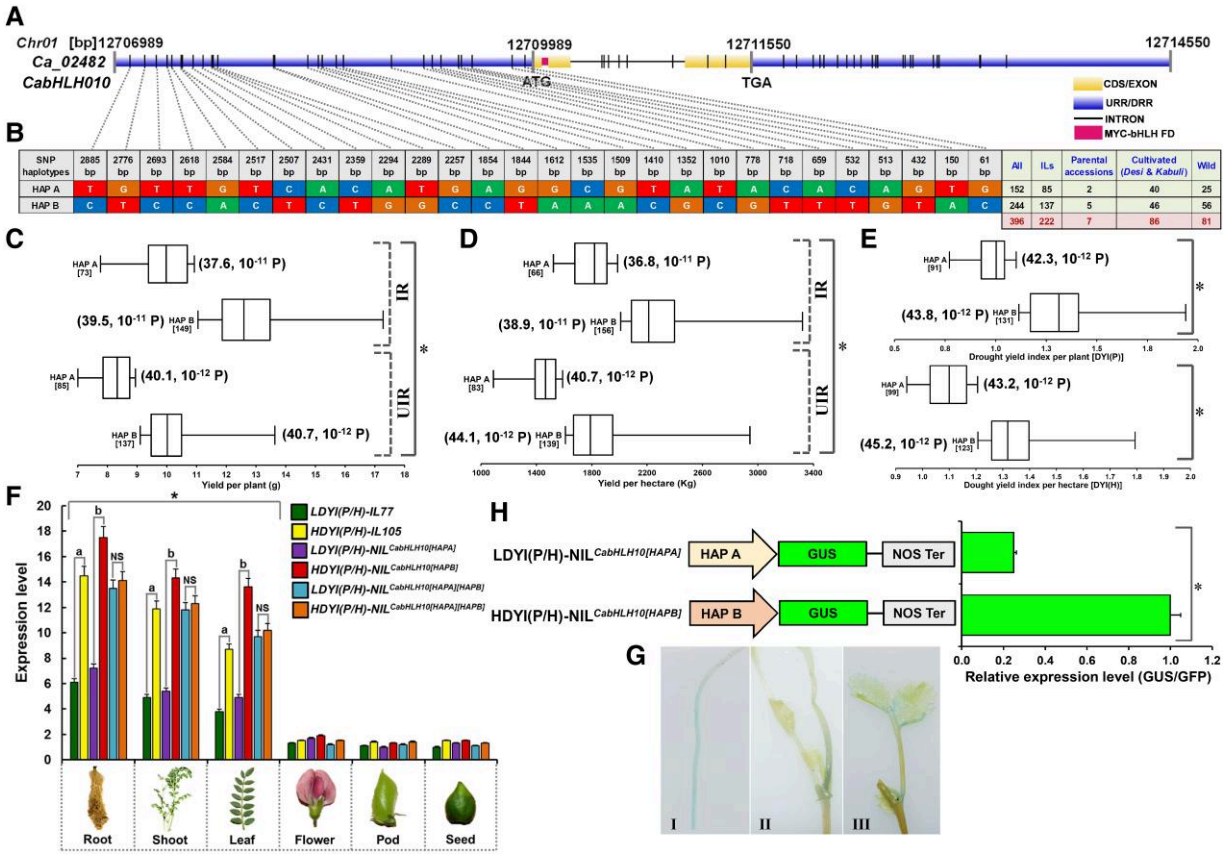

Figure 3 Superior natural haplotype of a *CabHLH10* transcription factor gene associated with drought tolerance, exhibit enhanced transcriptional activity/expression in the drought-tolerant lines. A–E, Gene haplotype-specific trait association mapping of *CabHLH10* in chickpea. A, Genomic organization and constitution of *CabHLH10* showing the distribution of 63 SNPs in different coding and non-coding sequence components of the gene. CDS: Coding sequence, URR/DRR: Upstream/downstream regulatory region, FD: Functional domain. B, The genotyping of 28 SNPs in the upstream regulatory region (URR) of a *CabHLH10* among 222 introgression lines (ILs) and seven accessions (used as parents to develop the ILs) as well as 86 cultivated *desi* and *kabuli* accessions and 81 wild *Cicer* accessions constituted two major haplotypes. C–E, Boxplots depicting the phenotypic variation for YP, YH, DYI(P) and DYI(H) traits in the said 222 ILs (association panel) represented by two haplotypes, HAP A and HAP B, demonstrating their significant association with low [LDYI(P/H)] and high [HDYI(P/H)] DYI, respectively. Box edges represent the upper and lower quantiles, with median values in the middle of the box. In Boxplots, Midline: Median; Box: Interquartile range (IQR) with box limits indicated by lower and upper quartiles of 25th and 75th percentiles, respectively; Whiskers: Minimal and maximal whisker data-points within 1.5-times of IQR from the first and third quartile, respectively. Digits in square brackets denote the number of ILs representing each class of haplotype associated with DYI. The YP, YH, DYI(P), and DYI(H) traits were evaluated in 222 ILs under both irrigated (IR) (unstressed) and unirrigated (UIR) (drought stress) conditions across all three years (over all years). *$P < 0.001$; Significant differences among unstressed and drought-stressed ILs belonging to individual haplotypes (HAP A and HAP B) estimated by one-way ANOVA and two-sided Wilcoxon test. F, Differential expression profile of low and high DYI(P/H)-associated *CabHLH10* gene haplotypes in the vegetative (root, shoot, and leaf) and reproductive (flower, pod, and seed) tissues of the corresponding haplotype-introgressed homozygous [LDYI(P/H)-NIL$^{CabHLH10(HAPA)}$ and HDYI(P/H)-NIL$^{CabHLH10(HAPB)}$] and heterozygous [LDYI(P/H)-NIL$^{CabHLH10(HAPA)(HAPB)}$ and HDYI(P/H)-NIL$^{CabHLH10(HAPA)(HAPB)}$] NILs and parental ILs [LDYI(P/H)-IL77 and HDYI(P/H)-IL105]. a, b represents the significant difference in expression level of gene haplotypes in HDYI(P/H) as compared to LDYI(P/H) NILs/ILs. Vertical error bars represent the mean ± standard deviation ($n = 3$, three independent biological replicates of each line and three technical replicates of each biological replicate). *Significant difference of expression level of gene haplotypes in the aforesaid vegetative tissues as compared to reproductive tissues at $P \leq 0.001$, estimated by Student's *t*-test. *x*- and *y*-axes indicate vegetative and reproductive tissues of NILs/ILs and relative expression level, respectively. C–F, Two-way ANOVA was performed with Genotype (G) and drought stress Treatment (T) as the two factors, and G × T as the Genotype and Treatment interaction. G: $P < 0.001$, T: $P < 0.001$ and G × T: $P < 0.01$. NS: Non-significant. G, Histochemical GUS staining of two weeks old *CabHLH10pro::GUS* transgenic chickpea plants showing organ-specific GUS signals in different tissues of I) roots, II) shoots, and III) leaves. H, Transient expression assay to determine the effects of low (HAP A) and high (HAP B) DYI(P/H) haplotypes constituted by the regulatory SNPs from the URR of a *CabHLH10* on its expression in the corresponding haplotypes-introgressed NILs. Left; the construct backbone with URR-SNP haplotypes (HAP A and HAP B) influencing the expression of their corresponding promoter-driven *GUS* (*β-glucuronidase*) reporter gene (CaMV 35S promoter as a control) regulating the expression of the GFP (green fluorescent protein used for normalization of transformation efficiency) reporter gene. Right; *Significant difference of GUS expression level in the chickpea leaves of HDYI(P/H)-NIL$^{CabHLH10(HAPB)}$ relative to LDYI(P/H)-NIL$^{CabHLH10(HAPA)}$ transiently transformed with corresponding URR-SNP haplotypes at $P \leq 0.001$, estimated by Student's *t*-test. Horizontal error bars represent the mean ± standard deviation ($n = 3$). HAP: haplotype, LDYI(P/H) and HDYI(P/H): low and high drought yield index per plant/hectare.

Marker (haplotype)-assisted selection develops *CabHLH10* haplotype-introgressed DYI-NILs

We investigated the role of *CabHLH10* gene-derived haplotypes (HAP A and HAP B) in controlling yield/productivity traits under drought stress, i.e. DYI(P/H) by developing haplotype-introgressed LDYI(P/H)-NIL$^{CabHLH10[HAPA]}$ and HDYI(P/H)-NIL$^{CabHLH10[HAPB]}$ NILs in chickpea. To accomplish this, haplotype-assisted foreground selection was performed using the SNPs linked/flanking to HAP A and HAP B haplotypes of a *CabHLH10* in the *CaqDYI(P/H)1.1* major QTL genomic region. Further, we chose a set of 1536 genome-wide SNPs that mapped uniformly on eight chromosomes among 26 positive recombinants (as identified by foreground selection) to perform subsequent genotyping and haplotype-assisted background selection across each of the advance generation back-cross mapping population until BC_6F_3. Finally, we specifically developed HAP A and HAP B haplotype-introgressed four LDYI(P/H)-NIL$^{CabHLH10[HAPA]}$ and three HDYI(P/H)-NIL$^{CabHLH10[HAPB]}$ NILs, respectively, with enhanced recovery of the parental recurrent genome (up to 98.8%–99.7%) by marker (haplotype)-assisted foreground and background selection (Supplemental Figures 11 and 12). Comprehensive phenotypic evaluation and characterization of the LDYI(P/H)- and HDYI(P/H)-NILs was performed using the soil cylinder culture (rainout shelter) under control unstressed and drought stress conditions to determine their agro-morphological responses towards drought. The HDYI(P/H)-NILs compared to LDYI(P/H)-NILs exhibited enhanced root biomass, including increased taproot length, primary lateral root number, and root surface area, with only a reduced (non-significant) yield penalty of fresh shoot weight (g), flower and pod number, and leaf branch number under drought stress (Figure 4, A–J; Supplemental Table 11). Histology-based morphometric measurements of the DYI-NILs (with five independent biological/technical replicates) revealed an overall decrease (~2.5-fold) in root cross-sectional area (RXSA) and total cortex area (TCA) and an increase (~2.5-fold) in total stele area (TSA) and metaxylem area (MXVA) in the drought-stress imposed root tissues of the HDYI(P/H)-NILs/ILs compared to their counterpart LDYI(P/H)-NILs/ILs (Figure 5, A–C). Overall decrease in RXSA and TCA with an increase in TSA and MXVA in the drought stress-imposed root tissues of HDYI- and LDYI-NILs/ILs is considered to be a common adaptation mechanism in response to drought (Prince et al., 2017). Increased TSA and MXVA have been reported to improve stomatal conductance, internal CO_2 capture, root hydraulic conductivity and water uptake, resulting in normal maintenance of shoot and root physiological processes as well as yield protection during drought stress in soybean and wheat (Kadam et al., 2015; Prince et al., 2017). Root morphological, physiological, and anatomical features are considered as the most important traits which have been phenotypically well-characterized, and further manipulated as well as optimized widely to demonstrate their potential to enhance crop yield and productivity in water-limited environments in many cereal (Zhu et al., 2010; Saengwilai et al., 2014; Kadam et al., 2015) and legume (Peña-Valdivia et al., 2010; Ramamoorthy et al., 2013; Prince et al., 2017) crops. These results overall infer that superior *CabHLH10* gene-derived haplotype (HAP B) has proficiency to enhance yield under drought stress in chickpea.

Enhanced transcriptional activity of a superior *CabHLH10* haplotype in DYI-NILs

To determine the functional importance of *CabHLH10* gene haplotypes (HAP A and HAP B), haplotype-specific differential expression profiling was performed in various vegetative and reproductive tissues of homozygous as well as heterozygous LDYI(P/H)- and HDYI(P/H)-NILs using the reverse transcription quantitative PCR (RT-qPCR) assay. Haplotype-specific expression profiling exhibited a pronounced expression (at least 8-fold up-regulation) of *CabHLH10* transcripts from both haplotypes (HAP A and HAP B) in the root, shoot, and leaf compared to flower, pod, and seed of homozygous and heterozygous DYI-NILs (Figure 3F). Interestingly, transcript from superior *CabHLH10* haplotype (HAP B) showed a higher expression (at least 2.5-fold upregulation) in the root, shoot and leaf of homozygous HDYI(P/H)-NIL$^{CabHLH10[HAPB]}$ compared to homozygous LDYI(P/H)-NIL$^{CabHLH10[HAPA]}$. However, no such significant difference in expression level was observed between heterozygous HDYI(P/H)-NIL$^{CabHLH10[HAPA][HAPB]}$ and LDYI(P/H)-NIL$^{CabHLH10[HAPA][HAPB]}$. To unravel the tissue-specific localization of *CabHLH10*, *in planta* promoter activity of this gene was investigated in the transgenic chickpea plants carrying *CabHLH10pro:GUS* construct, whereby the putative promoter of the *CabHLH10* was used to direct the expression of the β-glucuronidase (GUS) reporter gene. GUS staining of the transgenic chickpea plants (two weeks old) exhibited higher GUS activity in the root compared to shoot and leaf (Figure 3 G). Further, we performed a transient GUS expression assay in chickpea leaves through agroinfiltration of constructs-containing haplotype (HAP A and HAP B)-specific URR fragments, amplified from the corresponding homozygous HDYI(P/H)-NIL$^{CabHLH10[HAPB]}$ and LDYI(P/H)-NIL$^{CabHLH10[HAPA]}$, upstream of the *GUS* gene. *GUS* transcript level was significantly higher in the leaf harboring HAP B versus HAP A haplotypes in their URRs (Figure 3H), pointing to a positive correlation between promoter functionality and enhanced *CabHLH10* transcript accumulation (Figure 3, F–H). These findings further suggest that superior *CabHLH10* haplotype (HAP B) is transcriptionally more active compared to haplotype HAP A in the DYI(P/H)-NILs, possibly leading to enhanced yield/productivity during drought stress.

CabHLH10 transcriptionally regulates a known ABA-dependent drought-responsive gene, *CaRD22*, via a *trans*-eQTL

ABA is a major plant hormone that plays a vital role in plant response and tolerance to drought stress by modulating the

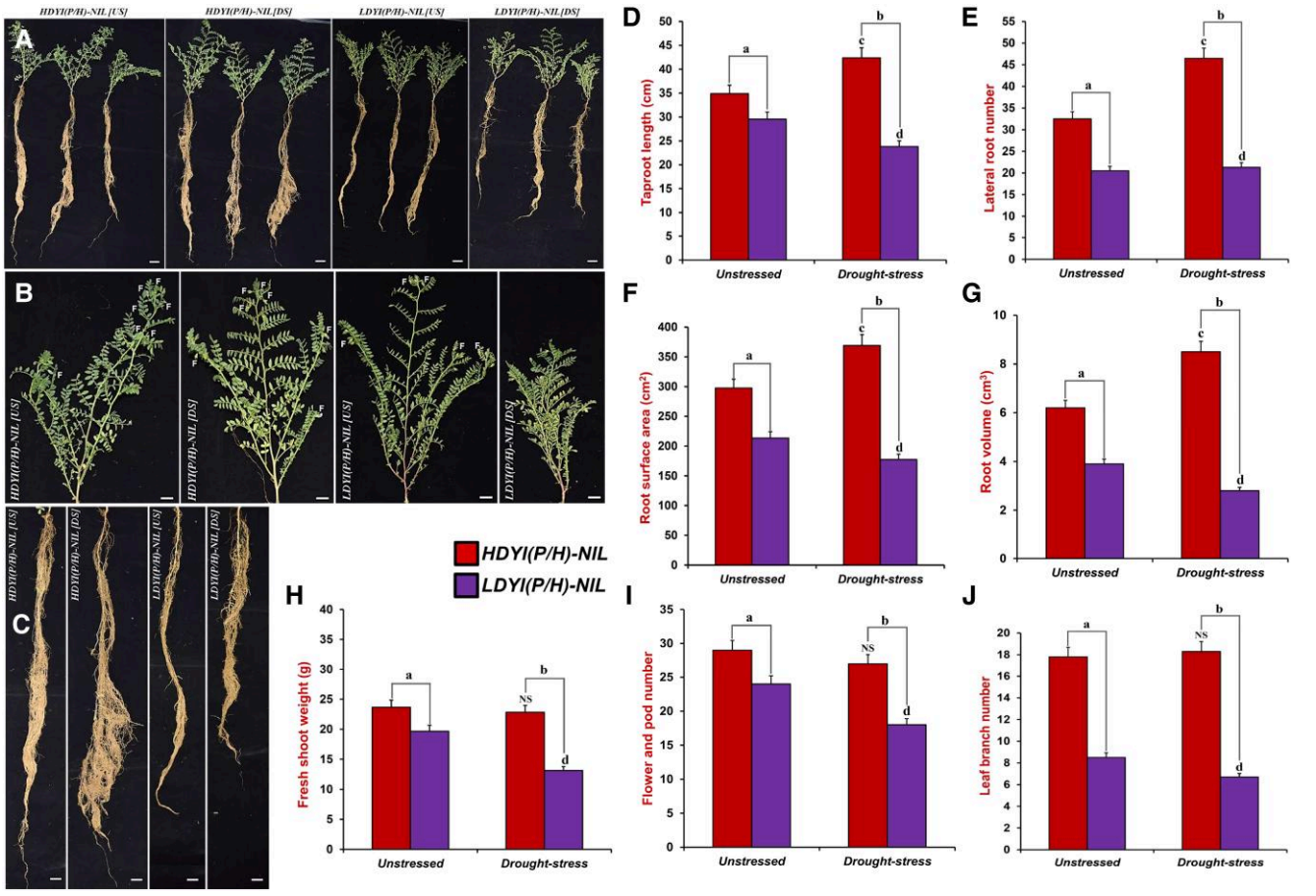

Figure 4 Field phenotyping demonstrated enhanced root physiological trait characteristics without compensating shoot growth/development in the drought-tolerant *CabHLH10* gene haplotype-introgressed lines during drought stress. A–C, Agro-morphological trait-based phenotyping of the roots and shoots of 45–60 days-old cylinder-soil-grown plants of high [HDYI(P/H)-NIL$^{CabHLH10(HAPB)}$] and low [LDYI(P/H)-NIL$^{CabHLH10(HAPA)}$] DYI-NILs evaluated at a rainout shelter under control unstressed (US) and drought stress (DS) conditions. D–J, Phenotypic variation for root and shoot agro-morphological traits including (D) taproot length (cm), (E) lateral root number, (F) root surface area (cm^2), (G) root volume (cm^3), (H) fresh shoot weight (g), (I) flower and pod number, and (J) leaf branch number in both low and high DYI(P/H) NILs. Significant difference in said root/shoot morphometric trait characteristics between HDYI(P/H)-NIL and LDYI(P/H)-NIL under US (a) versus DS (b) ($P < 0.001$, two-tailed *t*-test). Significant difference in root/shoot morphometric trait features during DS compared to US HDYI(P/H)-NIL (c) and LDYI(P/H)-NIL (d) ($P < 0.001$, two-tailed *t*-test). Vertical error bars represent the mean ± standard deviation ($n = 3$, 3 independent plants per NIL). Two-way ANOVA was performed with Genotype (G) and DS Treatment (T) as the two factors, and G × T as the Genotype and Treatment interaction. G: $P < 0.001$, T: $P < 0.001$ and G × T: $P < 0.01$. F: Flowers/pods grown in each NIL. NS: Non-significant. HAP: haplotype; LDYI(P/H) and HDYI(P/H): low and high drought yield index per plant/hectare. Scale bars: 1 cm. NIL: near isogenic line. The shoot (B) and root (C) images are from the same samples as depicted in (A).

expression of a cascades of drought- and ABA-responsive genes via ABA signalling (Abe et al., 2003). The expression of one such vital dehydration-responsive gene *RD22* (responsive to desiccation22) is also induced by ABA (Abe et al., 1997, 2003). A *MYC2*-type *bHLH* TF gene delineated in this study which is primarily known to be induced by ABA, binds to the *cis*-regulatory G-box elements and its variants on the promoter of a *RD22* gene and subsequently, induces its ABA-dependent drought response for imparting tolerance in crop plants (Abe et al., 1997, 2003; Shinozaki and Shinozaki, 2006, 2007; Dombrecht et al., 2007; Kazan and Manners, 2013). In this perspective, eQTL mapping was performed by integrating the differential expression profile of a known ABA-dependent drought-responsive gene, *CaRD22* during drought stress with the genotyping information of SNPs genetically mapped on chromosomes in an aforesaid RIL mapping population [LDYI(P/H)-IL77 × HDYI(P/H)-IL105] with contrasting DYI(P/H) traits. This analysis identified a major significant (LOD > 22.2) *trans*-eQTL [*CaeqDYI(P/H)1.1*] for a *CaRD22* gene which spans 2.8 kb genomic interval [12707104 bp (39.0 cM)–12709928 bp (39.5 cM)] on chromosome 1 (Supplemental Figure 14). The *CaRD22* gene (chromosome 4) was thus not congruent with its corresponding major eQTL (chromosome 1) in accordance with their mapped positions on chromosomes. This major eQTL for a *CaRD22* explained a total of 39.7%

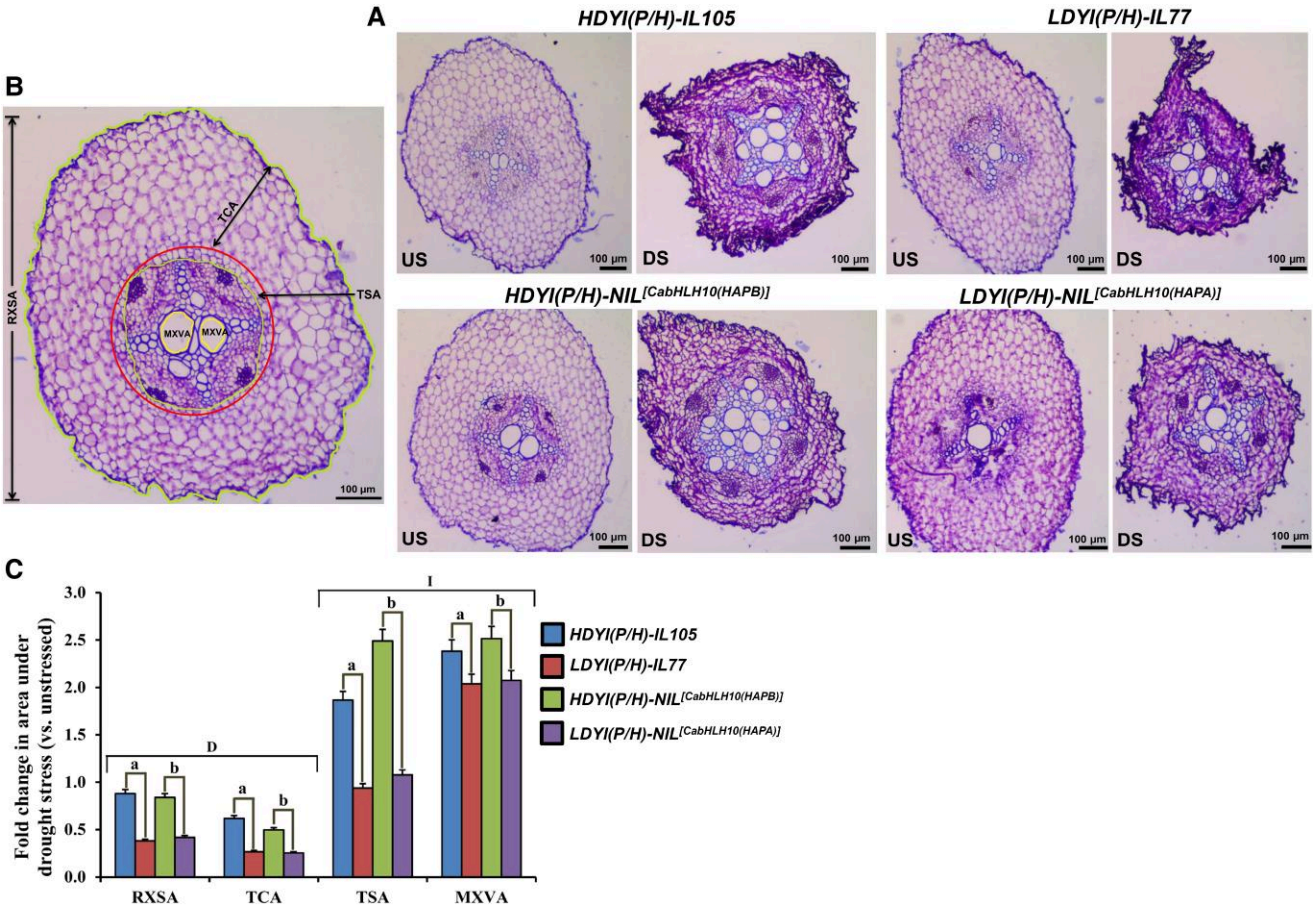

Figure 5 Histology-based phenotypic evaluation and characterization demonstrated improved root morphometric trait characteristics in the drought-tolerant *CabHLH10* gene haplotype-introgressed lines during drought stress. A, Microanatomical phenotyping and morphometric trait measurement of the unstressed (US) and drought-stressed (DS, 12 h moisture stress) root tissues of 20-days-old pot-soil-grown plants of high [HDYI(P/H)-NIL$^{CabHLH10(HAPB)}$] and low [LDYI(P/H)-NIL$^{CabHLH10(HAPA)}$] DYI-NILs and parental ILs [HDYI(P/H)-IL105 and LDYI(P/H)-IL77] at the vegetative stage. RXSA: root cross-sectional area; TCA: total cortex area, TSA: total stele area; MXVA: metaxylem vessel area (shown in B). Scale bars: 100 µm. C, Relative fold change of the four morphometric root characteristics in drought-stressed compared to unstressed root tissues of aforesaid high/low DYI-NILs and parental ILs. Decreases and increases in area w.r.t. control are denoted by "D" and "I," respectively. All lines were grown and phenotyped with at least five biological replicates under unstressed and drought stress conditions in a controlled environment. Error bars represent the mean ± standard deviation for each sample with five independent replicates ($n = 5$). a, b: Significant difference in HDYI w.r.t. LDYI ($P < 0.001$, two-tailed *t*-test). Two-way ANOVA was performed with Genotype (G) and drought stress Treatment (T) as the two factors, and G × T as the Genotype and Treatment interaction. G: $P < 0.001$, T: $P < 0.001$ and G × T: $P < 0.01$. HAP: haplotype. L/HDYI(P/H): low/high drought yield index per plant/hectare. NIL: near isogenic line. IL: introgression line.

variation in the expression of this gene for drought tolerance. Interestingly, the eQTL of said *CaRD22* gene was found to harbor a promising strong DYI(P/H) trait-associated *CabHLH10* gene (delineated in this study) on the chromosome 1 (Supplemental Figure 14) and thus both of these genes were found to be *trans*-regulated for controlling drought tolerance in chickpea. We reasoned that *CabHLH10* might physically binds to *cis*-regulatory elements in the promoter of *CaRD22*, which harbors the *trans*-eQTL, thereby inducing ABA-dependent drought tolerance in chickpea.

To test this hypothesis, we performed yeast one-hybrid assay and electrophoretic mobility shift assay (EMSA) and observed that *CabHLH10* binds specifically to three tandem repeats of a *cis*-regulatory G-box variant (CACGTG) in the promoter region of *CaRD22* (Figure 6, A–C). However, *CabHLH10* failed to bind into the created mutated form (TTCGAC) of this G-box element (Figure 6, A–C). Further, chromatin immunoprecipitation (CHIP)-based qPCR assay validated more prominent/efficient binding (16-fold enrichment relative to control IgG) of *CabHLH10* to the aforementioned G-box elements in both HDYI(P/H)- and LDYI(P/H)-NILs (Figure 6, A and D). An *Arabidopsis thaliana* protoplast-based transient transactivation assay revealed that *35S:CabHLH10* increased the expression (1.9-fold luciferase activity compared to control) of *CaRD22:LUC* (Figure 6, E and F). These findings indicate that *CabHLH10* transcriptionally regulate *CaRD22* via sequence-specific

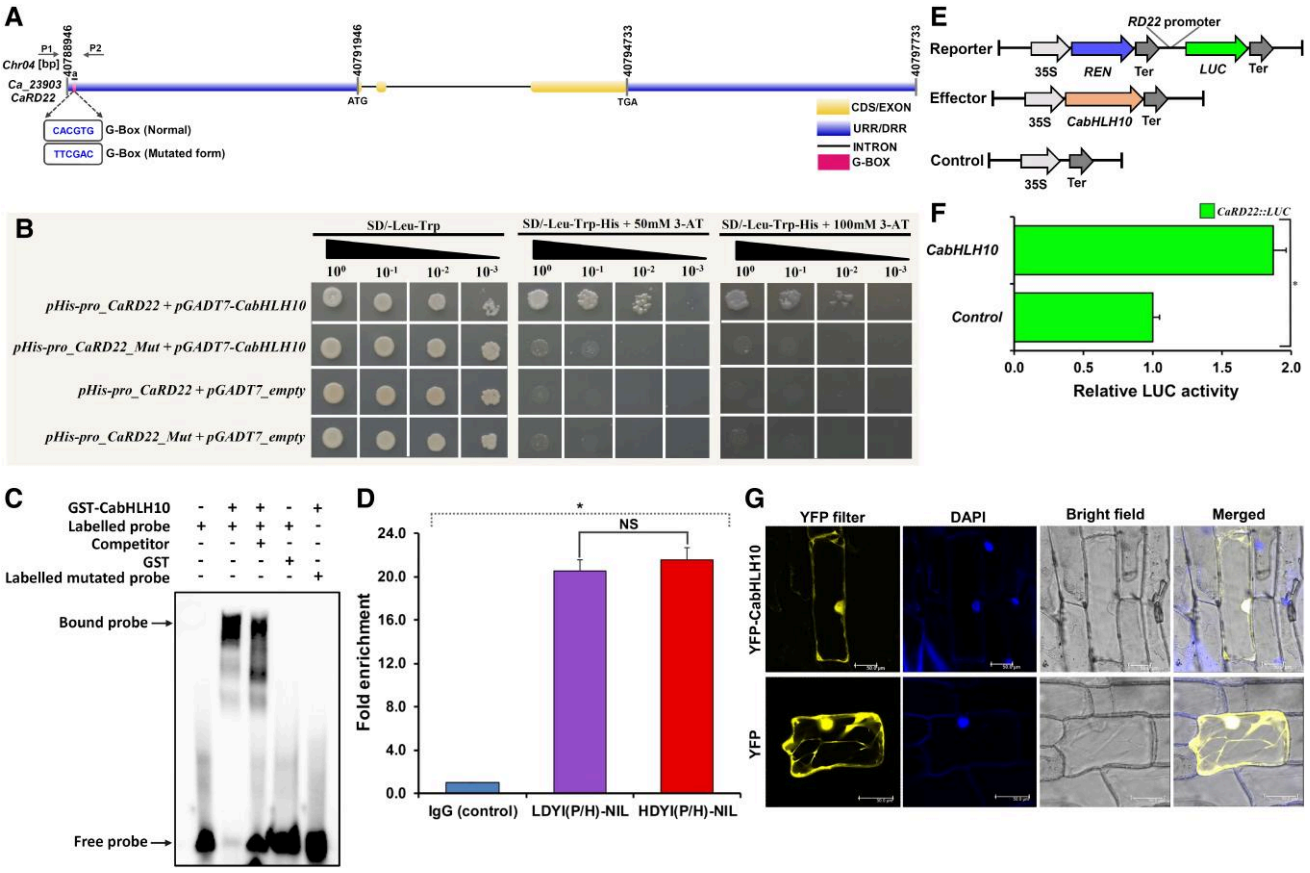

Figure 6 Nucleus-localized CabHLH10 interacts and transcriptionally regulates *CaRD22*, a known drought-responsive gene, to confer drought tolerance in chickpea. A, Schematic diagram of the genomic structural organization of *CaRD22*. The positions of forward and reverse PCR primers (P1 and P2) used for ChIP-qPCR analysis of *CaRD22* are indicated. Genomic DNA region (a) with the conserved G-box regions in the promoter (upstream regulatory region) of *CaRD22* used for yeast one-hybrid assay and electrophoretic mobility shift assay (EMSA) is indicated by a pink rectangle box. B, Interaction of *CabHLH10* with G-box element in the *CaRD22* promoter through yeast one-hybrid assay. Dilutions of transformed yeast cells were grown on different amino acid-deficient SD media with gradient 3-AT concentration. Growth of yeast cells cotransformed with pHIS2.1 vector consisting of G-box promoter element (*pHis-pro_CaRD22*) and *pGADT7* vector consisting of *CabHLH10* (*pGADT7-CabHLH10*) on selective medium indicates binding of CabHLH10 with the *CaRD22* promoter. The CabHLH10 is unable to bind to the mutated form of the G-box created in the *CaRD22* promoter (*pro_CaRD22_Mut*). C, EMSA showing interaction of CabHLH10 with G-box *cis*-regulatory elements in the *CaRD22* promoter. Biotin-labeled oligonucleotide probes from promoter elements displayed binding with GST-CabHLH10, while use of unlabeled probes competitively reduced labeled probe binding. Oligonucleotide probes from mutated G-box elements could not bind with GST-CabHLH10 and similarly GST alone could not bind to the promoter elements. D, ChIP-qPCR assay exhibiting binding of CabHLH10 to the G-box element in the promoter of *CaRD22* in vivo. Immunoprecipitation was performed with anti-CabHLH10 antibody. Immunoprecipitated chromatin was analyzed by RT-qPCR using primers indicated in (A). RT-qPCR enrichment was measured by normalizing to IgG = 1 and to the total input of each sample. Error bars represent the mean ± standard deviation for each sample with 3 independent replicates ($n = 3$). *Significance of LDYI(P/H) and HDYI(P/H) NILs as compared to internal control IgG in ChIP-qPCR assay ($P < 0.01$, two-tailed *t*-test). NIL: near isogenic line. NS: non-significant (E) Schematics depicting the effector and reporter plasmids used for the transient assay in Arabidopsis protoplasts. REN, Renilla luciferase; LUC, firefly luciferase. F, The relative LUC activity expressed by a reporter *CaRD22*Pro:LUC along with control (empty vector) or 35S:*CabHLH10* effector. Error bars represent the mean ± standard deviation for each sample with 3 independent replicates ($n = 3$). *Significant difference of LUC activity of *CabHLH10* as compared to control at $P \leq 0.01$ estimated by a two-tailed *t*-test. HAP: haplotype; L/HDYI(P/H): low/high drought yield index per plant/hectare. G, Sub-cellular localization of CabHLH10. Confocal microscopy images showing the localization of YFP-CabHLH10 (upper panel) and YFP alone (lower panel) which are transiently expressed in onion epidermal cells (under 2x CaMV35S promoter) through particle gun bombardment. DAPI (4′,6-diamidino-2-phenylindole) was used to stain the nuclei. Scale bars = 50 µm.

binding to the G-box *cis*-elements in its promoter region to confer ABA-responsive drought tolerance in chickpea. In onion epidermal cells harboring a *35S:YFP-CabHLH10* construct, *CabHLH10* was observed to be localized in the cytoplasm and the nucleus just like YFP control (Figure 6 G). The nuclear localization of *CabHLH10* further strengthens the conclusion that it is involved in transcriptional control of *CaRD22*. Overall, these findings highlight the roles of the genetic and physical interactions, as well as the transcriptional interplay, of *trans*-eQTLs in regulating *CaRD22* and

CabHLH10 expression to control drought tolerance possibly via ABA signaling in chickpea.

CabHLH10 induces drought tolerance by modulating ABA signaling

We explored whether drought and ABA stress is required for inducing *CabHLH10* leading to further *CaRD22*-mediated ABA-responsive drought tolerance in chickpea. For this, we primarily performed differential gene/haplotype-specific expression profiling of *CabHLH10* and *CaRD22* in the homozygous as well as heterozygous HDYI(P/H)- and LDYI(P/H)-NILs harboring *CabHLH10* haplotype introgression under unstressed (control), drought stress (12 h moisture stress), and exogenous ABA treatment (100 µM) conditions. Differential expression profiling using the RT-qPCR assay revealed higher expression of *CabHLH10* and *CaRD22* in both drought-stress and ABA-treated root and shoot compared to that of unstressed homozygous HDYI(P/H)-NILs as well as heterozygous HDYI(P/H)- and LDYI(P/H)-NILs. Remarkably, the enhanced expression of *CabHLH10* (at least 4.1-fold upregulation) and *CaRD22* (at least 4.2-fold upregulation) in the unstressed as well as the drought- and ABA-stress-imposed root and shoot of homozygous HDYI(P/H)-NIL$^{CabHLH10[HAPB]}$ compared to homozygous LDYI(P/H)-NIL$^{CabHLH10[HAPA]}$ was observed (Figure 7, A and B). We also observed enhanced expression of both *CabHLH10* and *CaRD22* under drought stress compared to unstressed homozygous NILs. However, no significant difference in the expression level of *CabHLH10* and *CaRD22* was obtained in the root and shoot between heterozygous HDYI(P/H)-NIL$^{CabHLH10[HAPA][HAPB]}$ and LDYI(P/H)-NIL$^{CabHLH10[HAPA][HAPB]}$ during drought- and ABA-stress (Figure 7, A and B). Global transcriptome profiling based on whole-genome transcriptome sequencing also revealed the upregulation of known/candidate genes underlying the ABA-responsive pathway in HDYI(P/H)-NILs versus LDYI(P/H)-NILs, especially in the root and shoot under drought- and ABA-stress (Figure 7 C; Supplemental Table 12). We further evaluated various agro-morphological traits of the HDYI(P/H)- and LDYI(P/H)-NILs using hydroponic, pot-soil, and phytagel medium (supplemented with/without 100 µM ABA) under controlled environment along with their estimated ABA content during drought and ABA stress. Agro-morphological evaluation revealed significant increase in root volume, with only a reduced (non-significant) yield penalty of fresh shoot weight in the HDYI(P/H)-NILs compared to LDYI(P/H)-NILs under drought- and ABA-stress (Figure 4, A–J; Supplemental Figure 15). Interestingly, ABA levels were also higher (at least 2.0-times) in the root and shoot of HDYI(P/H)-NILs compared to LDYI(P/H)-NILs under drought and ABA stress, indicating possible feedback of *CabHLH10* and *CaRD22* better equipping the plants for stress sensing (Figure 7 D). These observations overall indicate that ABA modulates *CaRD22*-mediated drought tolerance through *CabHLH10* regulation.

CabHLH10 transcriptionally activates yield-enhancing PE genes to confer higher yield/productivity during drought

We compared the effects of *CabHLH10* gene haplotypes on various seed yield component traits in HDYI(P/H)- versus LDYI(P/H)-NILs across multiple environments in the field under both unstressed and drought-stress conditions (Supplemental Table 13). Six high-yielding Indian *desi* and *kabuli* cultivated chickpea varieties and one wild progenitor, *Cicer reticulatum* accession used as parents to develop ILs, were also included in the analysis (Supplemental Table 1). HDYI(P/H)-NILs containing introgression of the superior *CabHLH10* gene haplotype (HAP B) exhibited many desirable seed yield attributes compared to the other lines, including higher yield per plant and yield per hectare (productivity) under both unstressed and drought-stress conditions, i.e. enhanced DYI(P/H) across all environments examined without compromising any desirable agronomic performance (Supplemental Figure 16; Supplemental Table 13).

We further performed a phenotypic evaluation of drought- and ABA-stress imposed HDYI(P/H)- versus LDYI(P/H)-NILs for major PE parameters that contribute to enhanced seed yield: chlorophyll content (CC; mg/g-FW), SPAD chlorophyll meter reading (SCMR), chlorophyll fluorescence (CF; Fv/Fm), CO_2 assimilation rate at increasing CO_2 concentration (CAR-CO_2↑; µmol $CO_2 m^{-2} s^{-1}$), and CO_2 assimilation rate at increasing light intensity (CAR-LI↑; µmol $CO_2 m^{-2} s^{-1}$). The HDYI(P/H)-NILs with improved root and shoot biomass had increased aforesaid PE parameters compared to their LDYI(P/H)-NILs counterparts during drought/ABA stress (Figure 8, A and B). The increased PE corresponded well with the upregulated expression of 16 previously reported (Basu et al., 2019) yield-enhancing PE-related chickpea genes in the drought/ABA-stress imposed HDYI(P/H)- versus LDYI(P/H)-NILs (Figure 8 C). Two strong yield-enhancing PE-associated genes encoding chlorophyll a/b-binding (CaCAB) protein and a basic leucine zipper (CabZIP) TF were strongly upregulated (at least 10-fold) in the HDYI(P/H)-NILs, especially under drought/ABA stress. A ChIP-based RT-qPCR assay further confirmed the notion that *CabHLH10* modulates the expression of two said strong PE-associated genes by specifically binding to the G-box *cis*-regulatory elements (CACATG) in their promoters (Figure 8, D–G). Besides, a major *trans*-eQTL [*CaeqDYI(P/H)1.1*] genomic region identified for two PE genes, *CaCAB* and *CabZIP* was found to harbor a strong DYI(P/H) trait-regulating *CabHLH10* TF delineated in this study and which further showed correspondence to an eQTL region detected for *CaRD22* on chromosome 1 (Supplemental Figure 14). This finding implies that *CabHLH10* activates the transcription of two strong yield-enhancing PE genes to increase efficiency of photosynthesis during drought stress in chickpea. We conclude that *CabHLH10* improves survival during drought stress as well as enhances yield/productivity of chickpea by modulating transcriptional regulation of *CaRD22* and PE genes in response to ABA signaling.

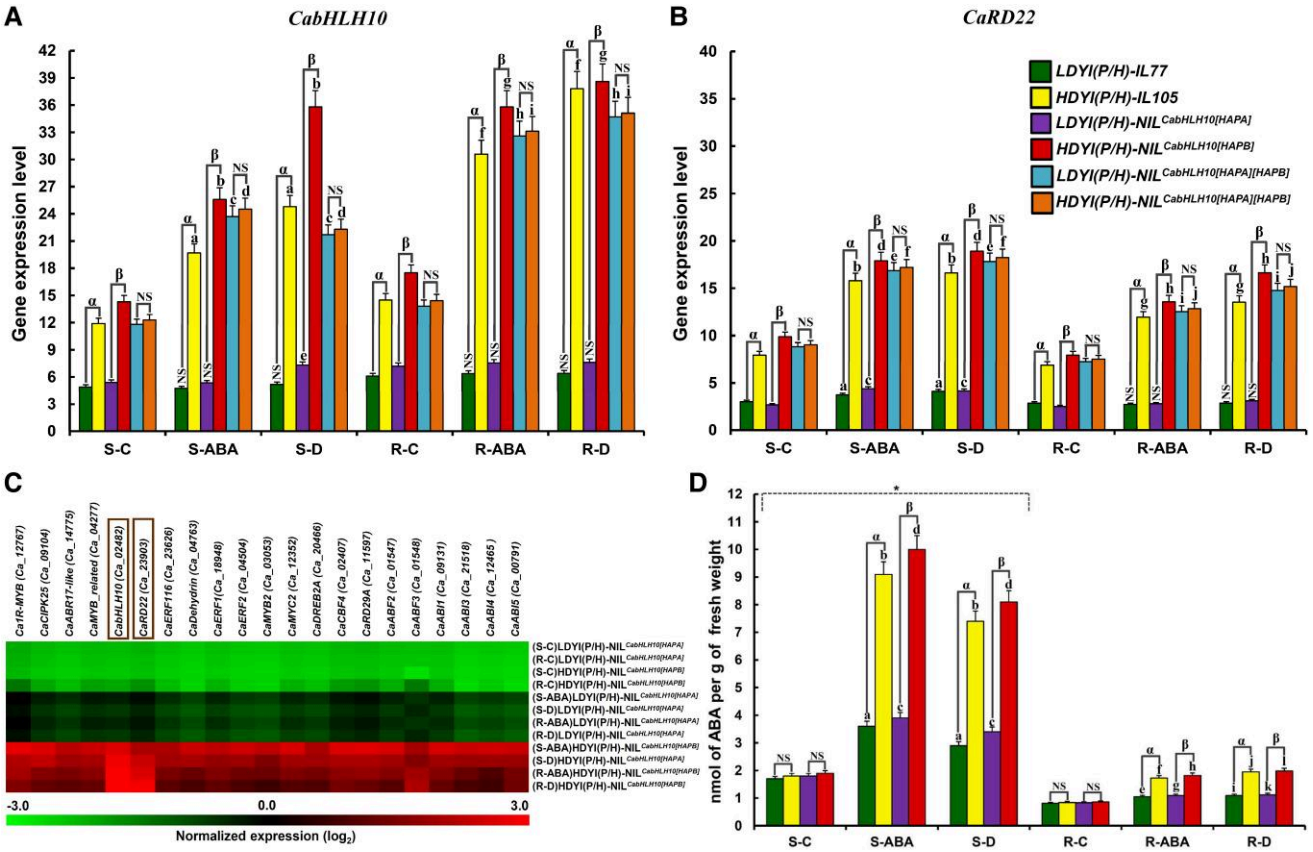

Figure 7 *CabHLH10* enhances drought tolerance by modulating transcriptional regulation of *CaRD22* in response to ABA signaling genes in chickpea. Differential expression profile of *CabHLH10* gene haplotypes (A) and its downstream dehydration-responsive gene *CaRD22* (B) in the control (unstressed) as well as drought (12 h moisture stress) and ABA (100 μM ABA) stress-imposed root and shoot tissues (20-d-old pot-soil-grown plants at the vegetative stage) of high and low DYI *CabHLH10* gene haplotype-introgressed homozygous [LDYI(P/H)-NIL$^{CabHLH10(HAPA)}$ and HDYI(P/H)-NIL$^{CabHLH10(HAPB)}$] and heterozygous [LDYI(P/H)-NIL$^{CabHLH10(HAPA)(HAPB)}$ and HDYI(P/H)-NIL$^{CabHLH10(HAPA)(HAPB)}$] NILs and parental ILs [LDYI(P/H)-IL77 and HDYI(P/H)-IL105]. Two-way ANOVA was performed with Genotype (G) and drought stress Treatment (T) as the two factors, and G × T as the Genotype and Treatment interaction. G: $P < 0.001$, T: $P < 0.001$ and G × T: $P < 0.01$. a–f and g–j: significant difference of *CabHLH10* gene haplotype expression in the drought/ABA-stress imposed shoots and roots, respectively, of high and low DYI-NILs/ILs as compared to its corresponding control unstressed tissues analyzed ($P < 0.001$, two-tailed *t*-test). Error bars represent the mean ± standard deviation for each sample with 3 independent replicates ($n = 3$). α, β: Significant difference in gene haplotype expression in the drought/ABA stress-imposed shoots and roots of HDYI w.r.t. LDYI ($P < 0.001$, two-tailed *t*-test). S-C/S-ABA/S-D: Shoot-control/shoot-ABA/shoot-drought, respectively. R-C/R-ABA/R-D: Root-control, root-ABA, root-drought, respectively. NIL: near isogenic line. IL: introgression line. NS: non-significant. *x*- and *y*-axes indicate the unstressed and drought/ABA stress-imposed root and shoot tissues of NILs/ILs and relative gene expression level, respectively. C, Differential expression profile of ABA-responsive known/candidate genes controlling drought tolerance in crop plants assayed through global transcriptome profiling of aforesaid (A, B) unstressed and drought/ABA-treated root and shoot tissues of homozygous NILs. The green, black, and red color scale at the bottom represents low, medium, and high levels of average normalized $\log_2$ signal expression value of genes in different tissues, respectively. The accessions/tissues and genes selected for expression profiling are indicated on right and upper part of expression map, respectively. Detailed information about the ABA-responsive genes is provided in Supplemental Table 12. D, Variation in ABA content (nmol) measured in 1 g fresh weight (FW) of aforementioned (A, B) unstressed and drought/ABA-stress imposed root and shoot tissues of homozygous NILs and parental ILs. a-d, e-h and i-l represent statistical significance in drought/ABA-stress imposed shoots and roots, respectively of NILs/ILs w.r.t. unstressed control ($P < 0.001$, two-tailed *t*-test). Error bars represent the mean ± standard deviation for each sample with 3 independent replicates ($n = 3$). α, β: Significance in HDYI w.r.t. LDYI ($P < 0.001$, two-tailed *t*-test). *Significance in shoots w.r.t. roots ($P < 0.001$, two-tailed *t*-test). HAP: haplotype. L/HDYI(P/H): low/high drought yield index per plant/hectare.

Overexpression of *CabHLH10* enhanced drought tolerance in chickpea and *Arabidopsis* transgenics by improving root and shoot agro-morphological traits

As previously described, introgression of a superior haplotype of *CabHLH10* into the ILs by haplotype-assisted selection improved root and shoot biomass and PE, consequently increasing its yield and productivity during drought without compromising its agronomic performance. To further investigate and gain more insights into the role of *CabHLH10* for drought tolerance, we generated *CabHLH10*-overexpresssing (*35S:CabHLH10*) transgenic chickpea and *Arabidopsis* plants. Significant increase in root biomass (≥ 2-fold), taproot length

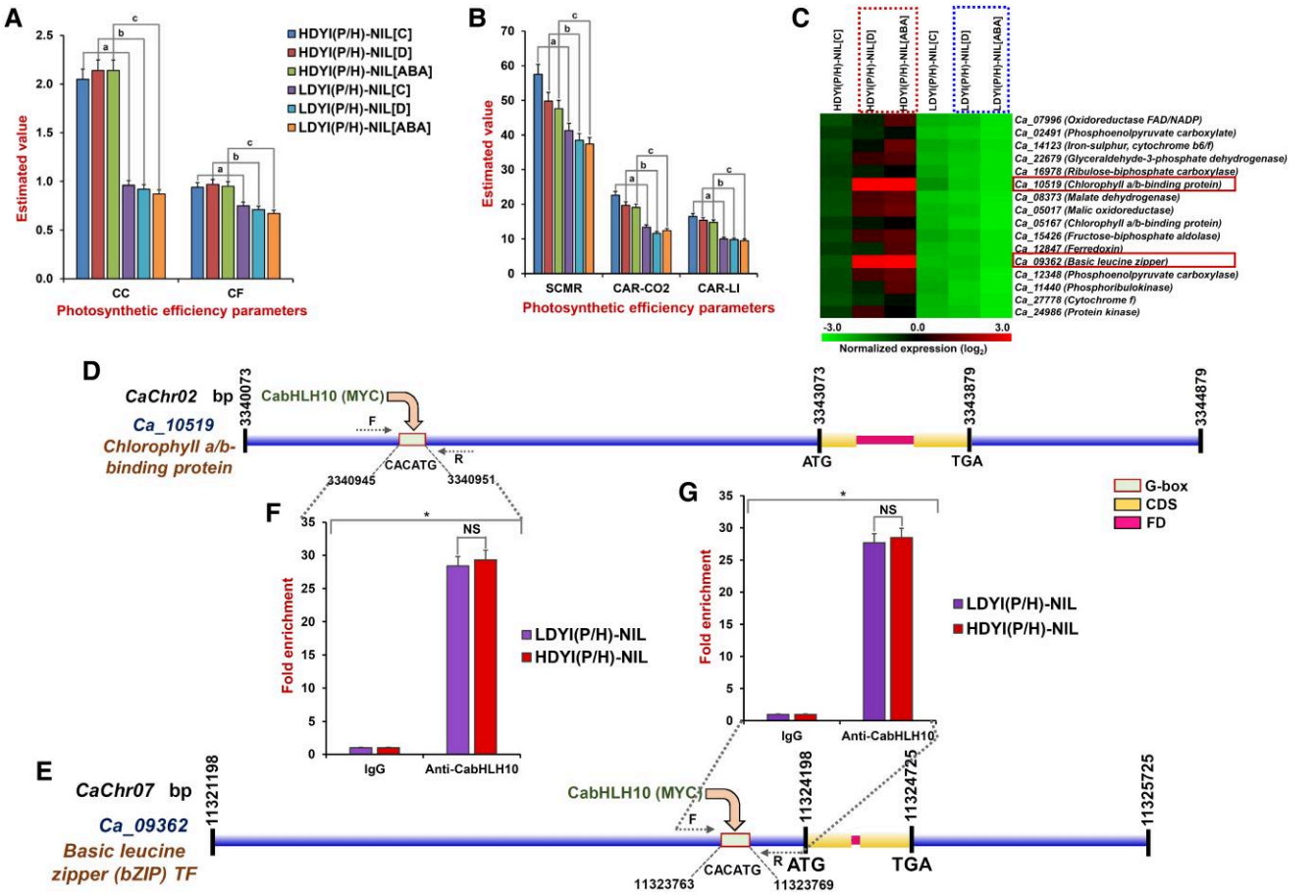

Figure 8 *CabHLH10* enhances seed yield and productivity by modulating transcriptional regulation of genes associated with high PE in chickpea. A-B, Bar plots illustrating the phenotypic variation for diverse PE trait parameters, including (A) CC (mg/g-FW) and CF (Fv/Fm), as well as (B) SPAD chlorophyll meter readings (SCMR), CO_2 assimilation rate at increasing CO_2 concentration (CAR-CO_2↑; µmol $CO_2 m^{-2} s^{-1}$), and CO_2 assimilation rate at increasing light intensity (CAR-LI↑; µmol $CO_2 m^{-2} s^{-1}$) under the unstressed control [C] as well as drought [D] and ABA stress-imposed high [HDYI(P/H)-NIL$^{CabHLH10(HAPB)}$] and low [LDYI(P/H)-NIL$^{CabHLH10(HAPA)}$] DYI *CabHLH10* gene haplotype-introgressed NILs. Vertical error bars indicate standard deviation with 3 biological replicates ($n = 3$). Two-way ANOVA was performed with Genotype (G) and drought stress Treatment (T) as the two factors, and G × T as the Genotype and Treatment interaction. G: $P < 0.001$, T: $P < 0.001$ and G × T: $P < 0.01$. a, b, c: significance in HDYI w.r.t. LDYI under the unstressed control, drought and ABA stress ($P < 0.001$, two-tailed *t*-test). C, Differential expression profile of 16 yield-enhancing PE chickpea genes in the control unstressed and drought/ABA-stress imposed shoots of aforesaid NILs. The green, black, and red color scale at the top represent low, medium, and high levels of average normalized $\log_2$ signal expression value of genes in the shoot tissue of NILs, respectively. The genes and NILs used for expression profiling are indicated on the right and upper part of the expression map, respectively. D and E, Gene structural organization depicting the accurate position (bp) of the G-box *cis*-regulatory elements (binding site for *CabHLH10*) in the 3-kb upstream regulatory regions (promoter) of two strong yield-enhancing PE genes encoding CaCAB protein (D) and basic leucine zipper (bZIP) transcription factor (TF) (E). CDS: coding sequence; FD: functional domain. (F, G) ChIP-qPCR assay confirmed the binding of CabHLH10 to the G-box *cis*-regulatory elements in the promoters of the two yield-enhancing PE genes, CaCAB protein (F) and bZIP TF (G). ChIP-qPCR was performed to amplify the immunoprecipitated DNA with forward/reverse primers (indicated by F and R in Figure D and E) targeting the G-box *cis*-regulatory element-binding sites in the PE genes. The ChIP-qPCR results are presented as fold changes by dividing the signals from ChIP with anti-CabHLH10 antibody by the IgG control. Vertical error bars represent the mean ± standard deviation for each sample with 3 independent replicates ($n = 3$). *Significance of gene enrichment in NILs as compared to internal control IgG ($P < 0.01$, two-tailed *t*-test). L/HDYI(P/H): low/high drought yield index per plant/hectare. NIL: near isogenic line. NS: non-significant.

(≥ 1.8-fold), lateral root number (≥ 2.0-fold), fresh shoot weight (≥ 2.0-fold), shoot height (≥ 1.9-fold), and relative water content (≥ 1.7-fold) under both unstressed and drought stress conditions in the transgenic chickpea lines compared to the wild-type (WT) plants was observed (Supplemental Figure 17). Under drought stress, the WT showed significant loss of shoot biomass (1.7-fold), whereas transgenic lines showed minimal loss (Supplemental Figure 17, G and H). *CabHLH10* expression was also significantly higher in the root (4.2-fold) and shoot (3.8-fold) tissues of transgenic chickpea lines (Supplemental Figure 17, J). Further, we demonstrated that overexpression of the

CabHLH10 in *Arabidopsis bHLH10* mutant improves the drought tolerance of the transgenic lines (Supplemental Figure 18). Under water-deficit stress (water withheld for 3-weeks), the survival rate of the mutant (15%) was significantly lower compared to the WT (66%) and transgenic lines (55%) after recovery (Supplemental Figure 18, A–C). Significant reduction (2.2-fold) in the relative water content (RCW) accompanied by faster rate of water loss of the mutant leaves was observed in the mutant compared to the WT and transgenic lines (Supplemental Figure 18, D and E). This suggests that *CabHLH10* functionally complements the *bHLH10* mutant indicating its functional role in conferring drought tolerance and that susceptibility to drought in the *bHLH10* mutant was caused by lack of *bHLH10* function. Thus, our overall findings corroborated well with the aforementioned results observed in the HDYI(P/H)-NILs containing the superior *CabHLH10* gene haplotype. We postulated that the enhanced drought tolerance and improved agro-morphological traits observed during drought stress were due to the overexpression of *CabHLH10* in the transgenic lines. The overall evidences further indicate that *CabHLH10* delineated in this study plays an important role in enhancing drought tolerance and yield in chickpea.

Discussion

An integrated next-generation genomics-assisted breeding strategy delineates functionally relevant *CabHLH10* TF gene enhancing yield/productivity in chickpea under drought stress

Improvement of yield and productivity is the ultimate target of crop improvement program in water-limited environments. Deciphering the molecular genetic basis of complex quantitative drought-tolerance trait and identification of potential molecular tags linked to drought-responsive QTLs/genes is vital for achieving enhanced yield and productivity during drought stress in chickpea. Here, we employed a genome-wide NGS-driven integrated genomic strategy involving high-resolution GWAS, gene-by-gene regional association analysis, QTL/fine-mapping, map-based cloning, molecular haplotyping, and haplotype-specific association analysis in an IL-based association panel and -mapping population (RILs/NILs) to genetically dissect seed yield traits in chickpea under drought stress, including DYI(P/H). This strategy successfully uncovered a promising *bHLH* TF gene, *CabHLH10*, of a drought-responsive major QTL and its derived superior natural haplotypes regulating the DYI(P/H) traits in chickpea. This goal was achieved quickly due to the use of ILs with multiple desirable genetic attributes, such as a high degree of genetic relatedness/homogeneity and a low level of population genetic structure, as well as strong heritability of quantitative yield traits under drought stress (Tsujimoto, 2001; Yano et al., 2016; Rockman and Kruglyak, 2009; Venuprasad et al., 2011; Zhang et al., 2012). These useful characteristics of ILs also allowed us to efficiently scan and exploit potential abiotic stress tolerance allelic variants from a wild *Cicer* gene pool with homogeneous genetic backgrounds of cultivated *desi* and *kabuli* chickpea for genomics-assisted crop improvement. The greater efficiency of these homogeneous IL-based genetic resources compared to commonly used natural association panels and mapping populations with heterogeneous genetic backgrounds allowed us to rapidly decipher the complex genetic architecture of quantitative yield traits under drought stress. The efficiency of our approach is also attributable to the greater utility of ILs for fine-mapping/map-based cloning and association mapping via the generation of more recombination events, ultimately leading to a reduction in the extent of LD and an overall increase in mapping resolution in chickpea, which is known for its narrow genetic base. Therefore, the integrated genomic strategy employed in this study could be useful for detecting non-spurious marker-trait association and causal genes governing important agronomic traits, thereby facilitating marker-assisted genetic improvement of chickpea and other crop plants.

Superior natural haplotype of *CabHLH10* improves drought tolerance and enhance yield/productivity in chickpea during drought by modulating ABA signaling and transcription of PE genes

To infer the functional importance of *CabHLH10* for drought tolerance, we deployed a gene haplotype-assisted foreground and background selection to precisely identify the most promising recombinants and to develop HDYI(P/H)- and LDYI(P/H)-NILs with introgressions of *CabHLH10* gene haplotypes (HAP B and HAP A) with excellent recovery (98%–99%) of the recurrent parental genome. Comprehensive phenotypic evaluation of HDYI(P/H)-NILs containing introgressions of superior *CabHLH10* gene haplotype (HAP B) exhibited improved root and shoot biomass contributing to yield enhancement under drought/ABA stress. The HDYI(P/H)-NILs harboring an introgression of the superior *CabHLH10* gene haplotype (HAP B) performed better than seven high-yielding Indian *desi* and *kabuli* cultivated chickpea varieties and a wild *C. reticulatum* accession, exhibiting enhanced yield and productivity during drought stress without compromising other desirable agronomic traits. The improved agronomic performance of the HDYI(P/H)-NIL is attributable to the selection of a superior HAP B gene haplotype derived from a superior drought-tolerant and high-yielding stable introgression line (IL105) with minimal pleiotropic/epistatic effects on other agronomic traits. Furthermore, enhanced recovery of the parental recurrent genome (up to 98.8%–99.7%) by haplotype-assisted selection, and the absence of linkage drag effects on other loci governing agronomic traits also minimizes the undesirable effects on other traits of agronomic importance in the developed drought-tolerant high-yielding NIL. To rule out the possibility of any negative undesirable effects of the said superior haplotype on other biotic stress, the developed drought-

tolerant, high-yielding NIL (HDYI(P/H)-NILs) are currently being evaluated in the National Chickpea Varietal Field Trials across different agro-climatic regions of India under optimal growth conditions. So far, the Field Evaluation Trials showed complete resistance of HDYI(P/H)-NIL to major chickpea diseases such as *Fusarium* wilt (*Races 1, 2, 4*) and *Ascochyta* blight as well as mild resistance to Collar rot, Dry root rot and Pod borer. With the completion of two-years of multilocation National Field Trials, the developed HDYI(P/H)-NIL may be released as an improved drought-tolerant, high-yielding chickpea variety with superior agronomic performance. Genomics-assisted breeding strategies are successfully being deployed for introgression of major genomic loci into multiple leading chickpea varieties resulting in development of multiple improved a/biotic stress tolerant varieties with higher yield under rainfed conditions in chickpea (Varshney et al., 2013b, 2014b; Pratap et al., 2017; Mannur et al., 2019; Bharadwaj et al., 2021). The overall evidences obtained from the genetically tailored *CabHLH10* introgressed marker-assisted breeding lines as well as chickpea and *Arabidopsis* transgenics clearly indicate that *CabHLH10* plays a vital role in enhancing yield under drought stress in chickpea.

Drought stress is known to activate ABA biosynthesis, which in turn induces the expression of a diverse array of drought-inducible genes in crop plants. The *MYC2*-type *bHLH* TF is an ABA and drought-responsive gene that regulates plant tolerance to drought by orchestrating various downstream drought/ABA-inducible genes as a transcriptional activator in the ABA signaling pathway (Abe et al., 2003). *MYC2* is known to specifically bind to the G-box elements in the promoter of *RD22*, a dehydration- and ABA-responsive gene, activating the drought-induced expression of *RD22* to confer ABA-dependent response and drought tolerance in crop plants (Abe et al., 2003). Here, we demonstrated that *CabHLH10* binds to the *cis*-regulatory G-box element in the promoter of *CaRD22* underlying a major *trans*-eQTL. Our study also assured that drought- and ABA-stress induces the expression of a *bHLH* TF gene, *CabHLH10* in chickpea (Figure 9) (Kazan and Manners, 2013). The enhanced expression of a natural superior *CabHLH10* gene haplotype (HAP B) in the root and shoot of HDYI(P/H)-NILs compared to their counterparts LDYI(P/H)-NILs during drought and ABA stress was observed (Figure 9). The enhanced accumulation of *CabHLH10* gene/haplotype-specific transcript and the interaction of *CabHLH10* with the *CaRD22* promoter potentially led to increased *CaRD22* expression in HDYI(P/H)-NILs compared to LDYI(P/H)-NILs (Figure 9). Thus, the higher expression level of the superior *CabHLH10* gene haplotype leads to the induction of its downstream gene, *CaRD22*, which helps the plant better adapt to drought conditions. However, no significant differences in the expression of both *CabHLH10* and *CaRD22* genes in LDYI(P/H)-NILs under drought/ABA stress was observed (Figure 7, A and B). We infer that because the drought sensitive LDYI(P/H)-NILs carry the introgression of the inferior HAP A haplotype inherited from the drought sensitive parental IL [LDYI(P/H)-IL77], therefore it does not seem to respond to drought or ABA stress, which is consistent with its reduced root and shoot physiological trait characteristics during drought stress (Figures 4 and 5). Interestingly, we also observed higher ABA levels in the HDYI-NILs during drought stress consistent with previous reports that several *bHLH* genes are involved in the induction of ABA biosynthesis for enhancing drought tolerance (Toledo-ortiz et al., 2003; Muhammad Aslam et al., 2022). Therefore, we postulated that the enhanced transcriptional activity of both *CabHLH10* and *CaRD22* in response to drought/ABA stress influence ABA biosynthesis, indicating possible feedback of both genes to better equip the plants for drought sensing and defense via the ABA-mediated signaling pathway (Xiong and Zhu, 2003; Zong et al., 2016). Summarily, *CabHLH10* functions as transcriptional activator of certain drought/ABA-inducible genes, including the *trans*-eQTL regulating *CaRD22* expression during drought stress in chickpea.

PE is a vital metabolic trait that directly contributes to crop grain yield since yield is determined by how efficiently a crop converts light energy into biomass through photosynthesis (De Souza et al., 2017). Therefore, enhancing PE is a desirable trait for enhancing crop yield during drought. Several PE parameters have widely been used to measure PE as an indicator of grain yield potential during normal and drought stress conditions in several crops (Guóth et al., 2009; Yamori et al., 2016; De Souza et al., 2017; Basu et al., 2019). The enhanced PE in HDYI(P/H)-NILs was accompanied by upregulated expression of yield-enhancing PE-associated genes in these HDYI(P/H)-NILs, especially under drought/ABA stress (Figure 9). Interestingly, two strong yield-enhancing PE genes, encoding CaCAB protein, and a bZIP TF, were transcriptionally regulated by a *trans*-eQTL harboring *CabHLH10* through its sequence-specific binding to the G-box *cis*-regulatory elements in their promoter regions, thereby enhancing overall PE and yield in the HDYI(P/H)-NILs during drought stress (Figure 9). Various genes/TFs in multiple crops are known to play roles in regulating photosynthesis-related metabolic pathways to increase the production of carbohydrates and their allocation to seeds, thereby enhancing seed yields and improving drought stress tolerance by increasing photosynthetic capacity (Oh et al., 2005; Zhang et al., 2008; Xu et al., 2012; Basu et al., 2019). Overall, the results suggests that *CabHLH10* improved root and shoot physiological traits as well as higher PE contributing to higher yield and productivity in the HDYI(P/H)-NILs under drought-stress conditions.

In conclusion, the HDYI(P/H)-NILs generated in this study, with superior allelic combinations of genes influencing DYI(P/H) traits, could serve as valuable donor genetic resources for developing drought-tolerant, high-yielding chickpea varieties with improved agronomic traits. Therefore, the molecular tags delineated in this study have the potential to

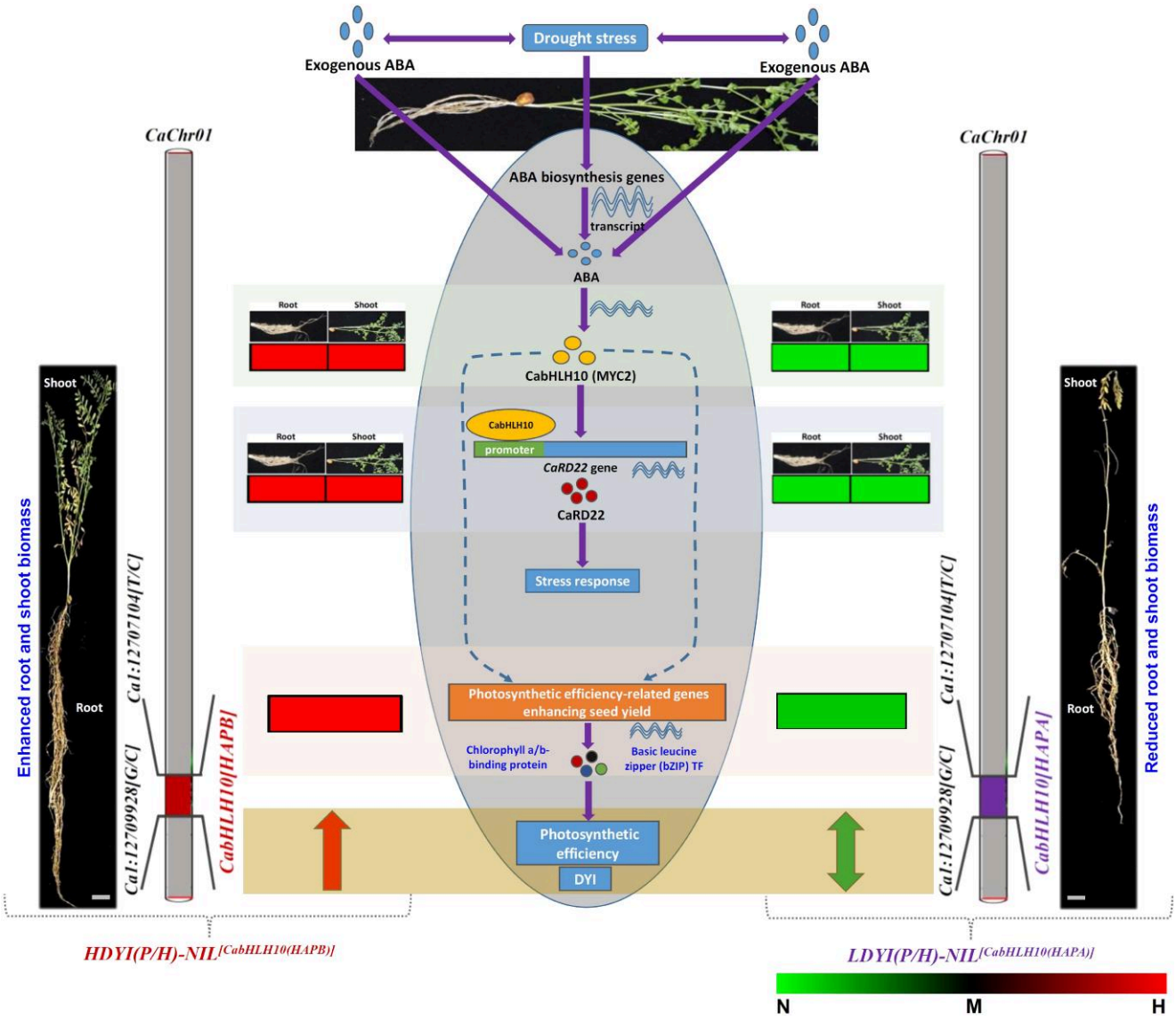

Figure 9 Schematic representation of the transcriptional regulatory role of *CabHLH10* in enhancing yield and productivity of chickpea during drought stress. The diagram depicts differential induction and higher expression of *CabHLH10*, *CaRD22*, and yield-enhancing PE genes in high [HDYI(P/H)-NIL$^{CabHLH10(HAPB)}$] versus low [LDYI(P/H)-NIL$^{CabHLH10(HAPA)}$] DYI *CabHLH10* gene haplotype-introgressed NILs during drought and/or ABA stress. Drought stress triggers the synthesis and production of ABA (in both HDYI and LDYI NILs) which induces the expression of *CabHLH10*. CabHLH10 then binds to the G-box cis-regulatory elements in the promoter of a known drought/ABA-responsive gene, *CaRD22*, indicating a possible transcriptional role for *CabHLH10* in enhancing *CaRD22* expression, potentially leading to upregulation of various downstream drought/ABA-responsive genes to impart confer ABA-dependent drought tolerance in chickpea. The green, black, and red color scale represents N (green): No change, M (black): Moderately upregulated and H (red): Highly upregulated expression of *CabHLH10* (upper panel), *CaRD22* (upper-middle panel), and yield-enhancing PE (lower middle panel) genes in the drought and/or ABA stress-imposed root and shoot tissues of NILs compared to the control. The figure also shows improved root and shoot biomass as well as PE resulting in higher drought yield index (DYI, lowermost panel) in high DYI- compared to low DYI-NILs, possibly due to the enhanced expression of yield-enhancing PE genes. The expression of two strong yield-enhancing PE genes (CaCAB protein and bZIP transcription factor as labeled in lower-middle panel) is induced by binding of CabHLH10 to the G-box *cis*-regulatory elements in their promoters as a transcriptional activator. The red and green colored arrows (lower panel) representing high and low PE/DYI, respectively. The NILs showing the introgressed regions of high (HAP B) and low (HAP A) DYI(P/H) *CabHLH10* gene haplotypes on chromosome 1, indicated on the extreme left and right, respectively. HAP: haplotype, L/HDYI(P/H): low/high drought yield index per plant/hectare.

uncover the genetic architecture and molecular mechanism underlying drought-tolerance traits that contribute to enhanced yield/productivity in chickpea. This information should drive translational genomic studies for crop improvement and the development of superior, genetically tailored, drought-tolerant chickpea cultivars with enhanced pod/seed yield and productivity to help ensure global food security.

Materials and methods

Development of introgression lines (ILs)

A set of 222 near-about homogeneous chickpea (*Cicer arietinum*) introgression lines (ILs) was selected from 32 advanced generation back-cross mapping populations (BC_3F_7) to constitute an association panel. These back-cross mapping populations were developed (following conventional phenotypic selection) by inter-crossing among seven *desi*, *kabuli* and wild chickpea accessions opting either as donor or recurrent parents in the back-cross breeding program initiated at the International Crops Research Institute for the Semi-Arid Tropics (ICRISAT), Patancheru, Hyderabad, India. The said seven accessions included four *desi* (ICC 4958, ICCV 93954, ICCV 10, and Annigeri), two *kabuli* (ICC 12968 and ICCV 92311) and one wild (*Cicer reticulatum*) (ICC 17160) chickpea with contrasting seed yield traits. The comprehensive strategies adopted to develop ILs are illustrated in Supplemental Figure 1.

Field phenotyping for yield traits under drought stress

The ILs belonging to an association panel were grown as per randomized complete block design (RCBD) in the experimental field with at least three replications for three consecutive years (2012–2014) at the ICRISAT (latitude/longitude: 17.1°N/78.9°E) under irrigated (IR, control unstressed) and unirrigated (UIR, water withheld drought stress) conditions during crop season (September to December) following Ramamoorthy et al. (2016, 2017). Subsequently, these ILs were phenotyped for major yield traits including pod number (PN), seed number (SN), 100-seed weight (SW), yield per plant (YP), yield per hectare (YH), drought yield index per plant [DYI(P)] and drought yield index per hectare [DYI(H)] both during IR and UIR conditions across three individual years (2012–2014) and over all years. PN, SN, SW, and YP traits were measured following previous methods (Singh et al., 2016; Shimray et al., 2017). Briefly, PN and SN for each IL were estimated by counting the average number of fully-matured pods and seeds per plant, respectively. The SW of each IL was calculated by measuring the average weight of 100-matured seeds at 10% moisture content. YP was calculated by weighing the average weight (g) of fully-matured dried seeds (at 10% moisture content) harvested from 10 to 12 representative plants of each IL. YH was measured by weighing the seed yield (kg) from all the plants of ILs with at least 60% of optimum plant stand in the field plots. DYI(P) and DYI(H) of each IL were estimated in accordance with Raman et al. (2012) following $DYI(P) = (YP)_{US}/(YP)_{DS}$ and $DYI(H) = (YH)_{US}/(YH)_{DS}$, respectively, in which US/DS indicates unstressed control IR versus drought stress UIR. The genetic inheritance characteristics of the traits were measured in an association panel by estimating the coefficient of variation, frequency distribution and Pearson's correlation coefficient (r) among ILs as described (Bajaj et al., 2015a, b; Upadhyaya et al., 2015). The analysis of variance (ANOVA) was employed to estimate the effect of genotypes (G) and phenotyping experimental years/environments (E) as well as their G × E interaction using SPSS v17.0 (http://www.spss.com/statsistics) (Srivastava et al., 2017). The broad-sense heritability [$H^2 = \sigma^2g/(\sigma^2g + \sigma^2ge/n + \sigma^2e/nr)$] was measured in accordance with σ^2g (genetic), σ^2ge (G × E) and σ^2e (error) variance with n (number of experimental years/environments) = 3 and r (number of replicates) = 3 as per Bajaj et al. (2015a).

Genotyping-by-sequencing assay

To construct a 3 × 96-plex Genotyping-by-sequencing (GBS) libraries, the genomic DNA isolated from 222 ILs (association panel) along with seven chickpea accessions (used as parents to develop ILs) was digested with *Ape*KI and ligated to adapters carrying unique barcodes. These libraries were pooled together and sequenced (100-bp paired-end) using an Illumina HiSeq2000 (Illumina Inc., USA) next-generation sequencing (NGS) platform (Elshire et al., 2011; Spindel et al., 2013; Kujur et al., 2015a, b, c). The reproducibility of the GBS assay was determined using the four *desi* (ICC 4958, ICCV 93954, ICCV 10, and Annigeri), two *kabuli* (ICC 12968 and ICCV 92311) and one wild *Cicer reticulatum* (ICC 17160) chickpea accessions as biological replicates (Supplemental Table 1). For sequence quality assessment, the raw FASTQ paired-end sequence reads (~100 base long) generated from each IL/accession were filtered using the recommended Illumina pipeline and NGS QC Toolkit v2.3 (Patel and Jain, 2012) to remove the low-quality including primer/adaptor contaminated sequence reads. The high-quality sequence reads (a *phred* score of ≥10) were further de-multiplexed based on their unique barcodes to extract reads of individual ILs/accessions. The de-multiplexed sequence reads of each IL/accession were aligned and mapped to the reference chickpea genome of *kabuli* (CDC Frontier; Varshney et al., 2013a; http://gigadb.org/dataset/100076] using Burrows-Wheeler Aligner (BWA) tool (Bowtie v2.1.0) with default parameters (Langmead and Salzberg, 2012) to generate the sequence alignment map (SAM) files. The SAM files were subsequently used for genome-wide mining of SNPs from ILs/accessions of chickpea.

Discovery and genotyping of genome-wide SNPs

To mine accurate SNPs from 222 ILs and seven parental chickpea accessions at a genome-wide scale, the SAM files were processed using the GBS pipeline of STACKS v1.0 (Catchen et al., 2013; http://creskolab.uoregon.edu/stacks) following Kujur et al. (2015a, b, c). In STACKS, a maximum-likelihood statistical model was used to screen all the valid and high-quality SNPs with no sequencing errors and SNP base quality of 20, supported by minimum sequence read-depth of 10. The structural and functional annotation of these SNPs on the diverse coding and non-coding sequence components of genes (.GFF file) and genome (chromosomes/pseudomolecules and unanchored scaffolds) of *kabuli* chickpea (Varshney et al., 2013a) were performed using the customized Perl scripts, single-nucleotide polymorphism effect

predictor (SnpEff v3.1 h; http://snpeff.sourceforge.net) and PFAM database v27.0 (http://pfam.sanger.ac.uk) as per Kujur et al. (2015a, b). Circos (Krzywinski et al., 2009) was employed to visualize the overall genomic distribution of SNPs with synonymous and non-synonymous substitutions based on their physical positions (bp) across eight chromosomes (pseudomolecules) of *kabuli* chickpea genome.

Molecular diversity and population genetic structure

To determine the molecular diversity and construct an unrooted neighbour-joining (NJ) phylogenetic tree (Nei et al. (1983) with 1000 bootstrap replicates), the genome-wide SNP genotyping information among 222 ILs (association panel) was analyzed in the PowerMarker (Liu and Muse, 2005) and MEGA7 (Kumar et al., 2016) following Kujur et al. (2015a, c). To infer the population genetic structure, genome-wide SNP genotyping information scanned from 222 ILs were analyzed in Bayesian clustering algorithm of STRUCTURE v2.3.4 (Pritchard et al., 2000) using the admixture and correlated allele frequency with the burn-in of 100,000 iterations, run-length of 100,000 and population number (K) 1–10. The optimal value of K was estimated using the *ad-hoc* approach of Pritchard et al. (2000) and *delta* K strategy of Evanno et al. (2005). Accordingly, various population genetic parameters including genetic divergence (FST) and degree of admixture among population groups of ILs were estimated.

LD decay

To estimate the genome-wide LD decay, the genotyping data of SNPs physically mapped on eight chickpea chromosomes were analyzed by a command (–r2 –ld-window 99999 –ld-window-r2 0) line interface of PLINK (Purcell et al., 2007) and the full-matrix approach of TASSEL (http://www.maizegenetics.net) (Bradbury et al., 2007) following Zhao et al. (2011) and Kujur et al. (2015c). The genome-wide LD decay was determined by plotting the average r^2 (correlation coefficient; frequency correlation among pair of alleles across a pair of SNP loci) estimated from the population (defined by population genetic structure) of a constituted association panel of ILs against the 50-kb uniform physical intervals across eight chromosomes. The statistical significance by comparing the r^2 values of LD across/within population group of ILs was performed employing the ANOVA interface tool of SPSS v17.0.

Genome-wide association study

For genome-wide association study (GWAS), the genome-wide SNP genotyping data was integrated with multi-environments (three individual years and over all years) replicated field phenotyping data of yield traits under control unstressed (IR) and drought stress (UIR) including PN, SN, SW, YP, YH, DYI(P), and DYI(H) as well as population structure (Q), kinship (K) and PCA (P) information of 222 ILs (association panel). The GAPIT (Lipka et al., 2012) and SPAGeDi 1.2 (Hardy and Vekemans, 2002) were used to estimate the PCA and K-matrix, respectively, among ILs. All these SNP genotyping and trait phenotyping as well as molecular diversity and genetic relatedness information obtained among 222 ILs were analyzed by a compressed mixed linear model (P + K, K, and Q + K) (Zhang et al., 2010) interface of GAPIT (Lipka et al., 2012) following Kujur et al. (2015a) and Kumar et al. (2015). To assure the accuracy of SNP marker-trait association in GWAS, the quantile–quantile (Q-Q) plot-based Benjamini and Hochberg false discovery rate (FDR cut-off $\leq$ 0.05) corrections were employed for multiple comparisons between observed/expected $-\log_{10}(P)$-value and adjusted *P*-value threshold of significance (Kujur et al., 2015a). Accordingly, SNP loci significantly associated with the traits were identified by individual year-wise and in three-years over all at a lowest FDR adjusted *P*-value (threshold $P < 1 \times 10^{-8}$) and highest R^2 in an association panel. The magnitude (R^2) of phenotypic variation explained (PVE) for the traits was measured by an FDR-controlling method of model with the SNP (adjusted *P*-value).

High-resolution QTL mapping

The GBS-derived genome-wide SNPs exhibiting polymorphism between two parental ILs [LDYI(P/H)-IL-77 and HDYI(P/H)-IL-105] (selected from an association panel) contrasting for yield traits under drought stress [PN, SN, SW, YP, YH, DYI(P), and DYI(H)] were screened. These SNPs were genotyped among 190 mapping individuals of a F_8 RIL population [LDYI(P/H)-IL-77 × HDYI(P/H)-IL-105] using Sequenom MALDI-TOF MassARRAY assay (http://www.sequenom.com) as per Saxena et al. (2014a, b). The high-throughput SNP genotyping data generated from a RIL mapping population was used to construct a genetic linkage map at the higher logarithm of odds (LOD) threshold (4.0–10.0) with Kosambi mapping function using JoinMap 4.1 (https://www.kyazma.nl/index.php/JoinMap) as described (Kujur et al., 2015b). A high-density genetic linkage map was constructed by integrating SNPs in accordance with their centiMorgan (cM) genetic distance and respective marker physical positions (bp) on eight linkage groups (LGs) (designated as LG1 to LG8)/chromosomes and further visualized by a Circos following Das et al. (2015).

For high-resolution QTL mapping, the genotyping data of parental polymorphic SNPs genetically mapped on a high-density genetic linkage map (eight LGs/chromosomes) were integrated with multi-environments (years) field phenotypic data of DYI(P) and DYI(H) as well as PN, SN, SW, YP, and YH traits of a RIL mapping population. This was performed using a composite interval mapping (CIM) function (LOD > 4.0 with 1,000 permutations and $P \leq 0.05$) of MapQTL 6 (Van Ooijen, 2009) as per Das et al. (2015) and Kujur et al. (2015b). The PVE (%) as well as positional and additive effect (evaluated by parental origin of favorable alleles) specified by each significant QTL were measured at a significant LOD ($P \leq 0.05$) following Bajaj et al. (2015b). The confidence interval (CI) of each significant major QTL peak was evaluated by using ±1-LOD support intervals (95% CI). The reaction norm plots of major DYI(P/H) QTLs detected

across three individual years and over all years were made and visualized by "rxnNorm" of R package.

Regional association analysis and molecular haplotyping

The genomic region (~100 kb) flanking the GWAS-derived SNP loci associated with DYI(P/H) traits and a strong DYI(P/H) trait-associated *CabHLH10* gene were targeted for regional association analysis and molecular haplotyping, respectively. For this, the selected genomic/gene regions were sequenced using the genomic DNA of 222 ILs (association panel) as well as 86 *desi* and *kabuli* chickpea accessions and 81 wild *Cicer* accessions employing the multiplexed amplicon sequencing protocol (as per manufacturer's instructions) of TruSeq Custom Amplicon v1.5 in Illumina MiSeq NGS platform (Supplemental Tables 1 and 9 and 10). The wild *Cicer* accessions included five annual wild species of primary and secondary genepools, namely *C. reticulatum* (16 accessions), *C. echinospermum* (8), *C. judaicum* (22), *C. bijugum* (19), and *C. pinnatifidum* (15) as well as one perennial accession of tertiary genepool *C. microphyllum*. The custom oligo probes targeting the selected genomic regions including coding DNA sequences (CDS)/exons and introns as well as 3 kb of each up/down-stream regulatory regions (URR/DRR) of genes were designed using Illumina Design Studio and synthesized further for their use in targeted multiplexed amplicon sequencing. The pooling of amplicons (an average size of 500 bp per reaction) into the custom amplicon tubes, construction of template libraries, normalization of the uniquely tagged pooled amplicon libraries and sequencing of generated clusters by Illumina MiSeq platform were performed as per Kujur et al. (2015b), Bajaj et al. (2015a) and Malik et al. (2016). The mapping of high-quality amplicon sequence reads onto reference *kabuli* chickpea genome (Varshney et al., 2013a) and detection of high-quality SNPs among ILs/accessions as well as their structural and functional annotation were carried out accordingly (Bajaj et al., 2015a; Kujur et al., 2015b; Malik et al., 2016). Subsequently, the constitution of SNP haplotypes in the sequenced genes and/or genomic regions and determination of SNP haplotype-based LD and domestication pattern including estimation of association potential of the haplotypes with DYI(P/H) traits were performed (Kujur et al., 2015a, b).

Fine-mapping and map-based cloning

To fine-map a major *CaqDYI(P/H)1.1* QTL identified by high-resolution QTL mapping, 380 mapping individuals of a F_2 population [LDYI(P/H)-$NIL^{CaqDYI(P/H)1.1}$ × HDYI(P/H)-$NIL^{CaqDYI(P/H)1.1}$] along with parental ILs were genotyped by amplicon resequencing-based SNPs using Sequenom MALDI-TOF MassARRAY (Saxena et al., 2014a, b). Subsequently, these SNP genotyping data were integrated with the field phenotyping information of yield traits generated from mapping individuals during control unstressed (IR) and drought stress (UIR) for high-resolution QTL mapping following aforesaid strategy.

For marker (haplotype)-assisted foreground selection, the SNPs flanking/tightly linked to the low and high DYI(P/H) haplotypes of a *CabHLH10* gene in the *CaqDYI(P/H)1.1* major QTL region were genotyped among mapping individuals of the back-cross population by the MALDI-TOF assay following Saxena et al. (2014a, b). Like-wise, for marker (haplotype)-assisted background selection, 1536 SNPs mapped uniformly across eight chromosomes of chickpea genome were genotyped in the selected recombinants (back-cross mapping individuals) using MALDI-TOF assay. For large-scale phenotyping of back-cross mapping population, the individuals were phenotyped for seed yield traits across multiple environments (three years) in the field as per RCBD with at least three replications under control unstressed and drought stress conditions following aforesaid strategies.

For progeny analysis, the homozygous recombinant and homozygous non-recombinant individuals derived from the low and high DYI(P/H) NILs were selected based on their genetic constitution and considering the recombination among SNPs flanking/tightly linked to the low and high DYI(P/H) haplotypes of a *CabHLH10* gene in the *CaqDYI(P/H)1.1* major QTL region. The selected recombinant and non-recombinant progenies were grown in the field as per RCBD with three replications across multiple environments (three years) and individual progenies were phenotyped precisely for yield traits under control unstressed and drought stress conditions. The significant variation of DYI(P/H) traits between selected recombinant and non-recombinant progenies were evaluated by a statistical one-tailed t-test. To evaluate the superiority of developed low and high DYI(P/H) gene haplotype-introgressed NILs for desirable agronomic traits, these lines along with parental ILs, six cultivated, and one wild *C. reticulatum* accessions were grown in the field as per RCBD (with three replications) across multiple environments (three years) under control unstressed and drought stress conditions, and further phenotyped for yield traits under drought stress.

Genome-wide identification and genomic constitution of bHLH TF genes

To identify diverse class of *bHLH* TF genes annotated from the *kabuli* chickpea genome (Varshney et al., 2013a), a genome-wide scan was performed through HMMER search (http://hmmer.org) with an E-value cutoff of 1e-05. Using the amino acid sequences of bHLH protein freely accessible at NCBI (https://www.ncbi.nlm.nih.gov), a hidden markov model (HMM) profile was made. The output amino acid sequences of HMM were further analyzed by INTERPRO (https://www.ebi.ac.uk/interpro) to ascertain the presence of functional bHLH domains in the identified *bHLH* genes. The genomic distribution and identity of *bHLH* genes was

determined in chickpea based on their lower to higher physical positions (bp) on the eight chromosome pseudomolecules and unanchored scaffolds of *kabuli* genome, and further visualized with a MapChart 2.2 (Voorrips, 2002).

Phylogeny of CabHLH10

The amino acid sequence of a *CabHLH10* was reciprocal BLAST searched against the protein sequences from the genomes of sequenced model dicot plant species, *Arabidopsis thaliana* (https://www.arabidopsis.org/) as well as other legumes including *Arachis duranensis*, *Arachis hypogaea*, *Arachis ipaensis*, *Cajanus cajan*, *Cicer arietinum*, *Glycine max*, *Phaseolus vulgaris*, *Medicago truncatula*, *Lotus japonicus*, *Trifolium pretense*, *Lupinus angustifolius*, *Vigna angularis*, and *Vigna radiata* (Phytozome; https://phytozome.jgi.doe.gov/pz/portal.html, Legume Information System; https://legumeinfo.org/ and NCBI; https://www.ncbi.nlm.nih.gov/). The presence of signature bHLH domains in the orthologous *bHLH* gene sequence-pairs were further assured by INTERPRO. Multiple sequence alignment of the bHLH functional domain in the amino acid sequence encoded by a *CabHLH10* gene with its *Arabidopsis* and legumes orthologs was performed using the BLOSSUM62 interface of CLUSTALW and accordingly an unrooted phylogenetic tree was constructed by a Neighbor-Joining (NJ) method and visualized in MEGA7 (www.megasoftware.net/, Kumar et al., 2016).

Reverse transcription quantitative PCR (Rt-qPCR) assay

Total high-quality RNA was isolated from shoots and roots of control unstressed as well as drought and ABA stress-imposed plants of low and high DYI(P/H) NILs/ILs using TRIzol (Sigma-Aldrich, USA) reagent and RNeasy MinElute Cleanup Kit (QIAGEN, USA) following manufacturer's instructions. The differential expression analysis was performed by the gene-specific primers (Supplemental Table 14) using the said tissues of the NILs/ILs following Bajaj et al. (2015a) and Upadhyaya et al. (2015). Briefly, 2 µg of high-quality DNase-treated RNA was used to synthesize cDNA by High-capacity cDNA Reverse Transcription Kit of Applied Biosystems (ABI, USA). The diluted cDNA (1:100 dilution) and 1X Fast SYBR Green Master Mix (ABI) as well as 200 nM of forward and reverse primers in a total reaction volume of 10 µl were used for amplification in the ABI7500 Fast RT-PCR system following manufacturer's instructions. Three biological replicates each with at least three technical replicates were used to calculate the mean relative expression level. An *elongation factor 1-alpha* (*EF1α*) gene was used as an endogenous control for normalization of the cDNA samples (Garg et al., 2010). The $2^{-\Delta CT}$ method was employed to determine the expression pattern of genes and two-tailed *t*-test was used to calculate the significant differences in expression levels of selected genes (Mukhopadhyay and Tyagi, 2015; Malik et al., 2016).

RNA-seq assay for global transcriptome profiling

For RNA-seq based global transcriptome profiling, the total high-quality RNA isolated from three independent biological replicates of root and shoot tissues of control (unstressed) as well as moisture and ABA stress-imposed 20-days-old pot-soil-grown seedlings of low and high DYI(P/H) NILs/ILs was used to constitute the paired-end cDNA libraries. All these libraries were sequenced using the Illumina HiSeq2000 platform to generate 100-base-long paired-end (PE) sequence reads for each NIL/IL sample. The raw Fastq sequences were filtered by NGS QC Toolkit v2.3 to discard the low-quality reads and further accessed for various quality parameters to be considered as high-quality sequence reads. The high-quality sequence reads were subsequently mapped on the reference *kabuli* chickpea genome (Varshney et al., 2013a) using TopHat v2.0.0 with default parameters. The mapped sequences of each NIL/IL sample were analyzed in Cufflinks v2.0.2 to obtain the normalized estimation of gene expression based on FPKM (fragments per kilobase of transcript per million mapped reads). Hierarchical clustering and PCA were performed employing corrplot and prcomp utilities of R package. The differential expression between all pairs of NIL/IL samples was estimated using Cuffmerge and Cuffdiff as per Srivastava et al. (2016). The genes exhibiting a difference of at least two-fold expression change between two given experimental NIL/IL samples with corrected *P*-value ≤ 0.05 after analyzing FDR (q-value) ≤ 0.05 were considered significant to be differentially expressed and visualized with a heat map using a MultiExperiment Viewer (MeV, http://www.tm4.org/mev). The stage-specific/preferential genes expressed in the NILs/ILs were identified using SS scoring algorithm as per Zhang et al. (2015). The higher value of SS score with the maximum expression level of a gene in a particular stage as compared to that of other stages analyzed signifies the more specific gene expression at that stage.

eQTL mapping

For eQTL mapping, the differential expression profiling of *CaRD22*, *CaCAB*, and *CabZIP* genes were performed in the control unstressed and drought stress-imposed root and shoot tissues of parental NILs and 380 individuals of a F_2 mapping population [LDYI(P/H)-$NIL^{CaqDYI(P/H)1.1}$ × HDYI(P/H)-$NIL^{CaqDYI(P/H)1.1}$] through RT-qPCR assay (as described) using primers enlisted in Supplemental Table 14. The Pearson correlation coefficient (r) with a statistical significance $P \leq 0.05$ was used to estimate the correlation and significant difference of expression level of genes with drought tolerance. The differential expression level data of *CaRD22*, *CaCAB*, and *CabZIP* transcripts (as a phenotype) and genotyping data of SNPs (as a genotype) genetically (cM) mapped on eight chromosomes were analyzed using the CIM function of interval mapping (threshold of significance LOD > 3.0 with 1000 permutations and $P \leq 0.05$) of MapQTL 6. The major eQTL identified was further assured by QTL window

interface module of QGene 4.3 (Joehanes and Nelson, 2008) as per Bajaj et al. (2015a) as well as using the generalized linear model (GLM) of TASSEL and multiple regression method of Melo et al. (2019). Accordingly, the position (cM) of a major drought-responsive eQTL regulating the relative gene expression level of *CaRD22*, *CaCAB*, and *CabZIP* for the drought tolerance was determined and visualized with "rxnNorm" of R package.

Transient expression analysis

For transient gene haplotype-specific expression assay, the upstream regulatory (promoter) of low and high DYI(P/H) haplotypes constituted from a *CabHLH10* gene were amplified from the DNA of corresponding low and high DYI(P/H) haplotype-introgressed NILs and parental ILs using specific primers (CabHLH10p_F and CabHLH10p_R) enlisted in Supplemental Table 14. These were further cloned into a binary plasmid vector pCAMBIA1301 at the *Bam*HI/*Sal*I restriction sites to drive expression of beta-glucuronidase (GUS) reporter protein. *Agrobacterium tumefaciens* strain EHA105 containing this recombinant plasmid along with another plasmid vector pCAMBIA1302 expressing green fluorescent protein (GFP) reporter gene (used for normalization of transformation efficiency) were agro-infiltrated into the young leaves of two months old seedlings of a *desi* chickpea accession ICCV 93954 following Dwivedi et al. (2017). The normalization of transformation efficiency and estimation of GUS activity from the *CabHLH10* gene/haplotype constructs were made using the RT-qPCR assay in accordance with Dwivedi et al. (2017). Three biological replicates each with at least three technical replicates of each gene/haplotype construct were assayed for transient expression study.

Yeast one-hybrid assay

The CDS of a *CabHLH10* gene amplified from the high DYI(P/H) gene haplotype-introgressed NILs were cloned in a Gateway vector pENTR™/D-TOPO® (Invitrogen, USA), and were subsequently mobilized into the gateway compatible pGADT7 (pDEST-GADT7) vector using LR clonase II enzyme mix (Invitrogen, USA) according to manufacturer's instructions. Three tandem repeats of wild-type G-box (CACGTG) and mutated G-box (TTCGAC) *cis*-regulatory elements in the URR of a *CaRD22* gene were generated by annealing forward and reverse oligonucleotides. The annealed fragments were further cloned in *EcoR*I-*Spe*I sites of pHis2.1 vector and their presence in the plasmids were confirmed by sequencing as per Kujur et al., (2013). Detailed primer and oligonucleotide sequence information are enlisted in Supplemental Table 14. pHis2.1 vector cloned with normal and created mutated G-box *cis*-regulatory elements were transformed separately with CabHLH10-pGADT7 in the yeast strain Y187 and checked for yeast growth along with other controls on different dropouts with or without various concentrations of 3-AT.

Transient transcriptional activation assay

For transient expression study, the full-length CDS of a *CabHLH10* gene/haplotype was amplified using the cDNA of a high DYI(P/H) *CabHLH10* gene haplotype-introgressed NILs using gene-specific primers (CabHLH10pRT_F and CabHLH10pRT_R) enlisted in Supplemental Table 14. The amplified CDS was then cloned into *Kpn*I and *Bam*HI sites of pRT107 vector to constitute an effector construct [35Spro:*CabHLH10*]. The URR (promoter region upstream to the translation start codon ATG) of a *CaRD22* gene targeting normal (CACGTG) G-box *cis*-regulatory element was amplified from the NILs and cloned into *Sal*I and *Bam*HI sites of pGreenII 0800-LU538C vector to constitute the reporter construct using specific primers (CaRD22pGreen_F and CaRD22pGreen_R) enlisted in Supplemental Table 14. Subsequently, the said effector and reporter constructs were co-transfected into the isolated *Arabidopsis* mesophyll protoplasts through PEG transformation following Sheen (2001) and Tian et al. (2017). A *Renilla* luciferase (*REN*) gene directed by cauliflower mosaic virus (CaMV) 35S promoter harboring in the pGreenII 0800-LUC vector was used as an internal control to measure the Firefly LUC and REN activities by a Dual-Luciferase reporter assay kit of a GloMax 20/20 luminometer (Promega, USA). Accordingly, the LUC/REN ratio was estimated by normalizing the activities of LUC to REN. Three biological replicates each with at least three technical replicates representing individual gene haplotype constructs were assayed for transient transcription assay.

ChIP qPCR assay

For the ChIP RT-qPCR assay, the NILs introgressed with high DYI(P/H) *CabHLH10* gene haplotypes were used to isolate nuclei in order to immunoprecipitate the sonicated chromatin suspension with protein–DNA complex by Anti-CabHLH10 antibody (Cell Signaling Technology, USA) as described (Sun et al., 2015; Tian et al., 2017). The chromatin precipitated with IgG (Merck-Millipore, USA) was used as a control in ChIP-qPCR profiling. Three biological replicates each with at least three technical replicates representing individual haplotypes were assayed for ChIP-qPCR assay. To perform ChIP-qPCR, the forward and reverse primers specific to *CaRD22*, *CaCAB* and *CabZIP* enlisted in Supplemental Table 14 were used.

ABA quantification

For estimation of ABA concentration, the control (unstressed) and ABA stress-imposed root and shoot tissues of 20-days-old pot-soil-grown seedlings of low and high DYI(P/H) NILs/ILs were harvested and stored at −80°C until further use. For ABA extraction, the samples were grounded into fine powder with liquid nitrogen. Subsequently, 50–100 mg of frozen tissues were analyzed on an Agilent 6530 Accurate Mass Q-TOF LC/MS (Agilent Technologies Inc., USA) with a MassHunter Qualitative Analysis software (version B.05.00) following Dave et al. (2011), Miyazaki et al. (2014) and Pang et al. (2017).

Three biological replicates each with at least three technical replicates were used for ABA estimation study.

Root histological assay

The low and high DYI(P/H) NILs/ILs were used for root histological assay. Five biological and three technical replicates from both control unstressed and dehydration/moisture stress-imposed root tissues of 20-days-old pot-soil-grown seedlings of said NILs/ILs were collected for root histological studies. Tap roots representing 1 cm above the tips of these NILs/ILs were cut, harvested, and washed. The root sections were further fixed, dehydrated, and embedded in paraplast and prepared for microtomy following Ranjan et al. (2017). Paraffin root sections (8 μM) were dissected using rotary microtome (Leica Biosystems, USA) and stained with 0.2% (w/v) toluidine blue (Sigma-Aldrich, USA). Images of the root sections were captured using light microscope (Leedz Micro Imaging Limited, UK) with 10 × 10 magnification (100X). Root anatomical analysis was performed using ImageJ 1.31 v (http://rsb.info.nih.gov/ij/) (Schindelin et al. 2015). The root morphometric parameters including total stele area (TSA), total cortex area (TCA), root cross-sectional area (RXSA), and meta xylem vessel area (MXVA) were measured in both control unstressed and stress-imposed plants of said NILs/ILs as described (Prince et al., 2017).

Electrophoretic mobility shift assay (EMSA)

To ascertain the binding of CabHLH10 to the *cis*-regulatory elements of the *RD22* promoter, GST-CabHLH10 (*CabHLH10* cloned in pGEX-4T1 at *Eco*RI/*Sal*I sites) was expressed in the bacterial BL21 cells and purified using Glutathione-Agarose (Thermo Scientific, USA). The oligonucleotide probes corresponding to G-box *cis*-regulatory element (native and mutated form, as used in yeast one hybrid) were labeled by the Biotin 3' End DNA Labeling Kit (Thermo Scientific). EMSA was performed using LightShift Chemiluminescent EMSA Kit (Thermo Scientific) according to the manufacturer's protocol. Biotin-labeled probes were incubated with GST-CabHLH10 or GST at room temperature for 20 min. The free probes and protein-probe complexes were electrophoresed on 6% polyacrylamide gel and further transferred on nylon + membrane. The biotin-labeled DNA was detected through chemiluminescence. Biotin-unlabeled probes were used as competitors in EMSA. Detailed primer sequence information is enlisted in Supplemental Table 14.

GUS promoter assay

For generation of promoter:GUS transgenics, 1.5 kb of the *CabHLH10* promoter was amplified from the genomic DNA of NILs introgressed with high DYI(P/H) *CabHLH10* gene haplotype, using specific primers (pCabHLH10_gus_Fand pCabHLH10_gus_R) enlisted in Supplemental Table 14. The amplified fragment was then cloned into Gateway pENTR™/D-TOPO® vector (Invitrogen, USA), and then mobilized into the binary vector pGWB3, upstream of the *β*-glucuronidase synthase (GUS), using LR clonase II enzyme mix (Invitrogen, USA) according to manufacturer's instructions. The resulting recombinant construct (*CabHLH10*$_{pro}$:*GUS*) was introduced into *Agrobacterium tumefaciens* strain GV3101, which was subsequently used to transform chickpea accession Pusa 362 (*desi*) via cotyledons/seeds explants by *in planta Agrobacterium*-mediated transformation methods following Chakraborti et al. (2006).

Histochemical GUS staining was performed using 5-bromo-4-chloro-3-indoxyl-beta-D-glucuronide (X-gluc, Biosynth, Staad, Switzerland) as a substrate, following the methods of Jefferson et al. (1987) and Khandal et al. (2020). To evaluate the promoter activity, two weeks old chickpea seedlings were vacuum infiltrated with GUS staining solution (50 mM sodium phosphate buffer, pH 7.0, 10 mM EDTA, 0.1% [v/v] Triton X, 0.5 mM ferrocyanide, 0.5 mM ferricyanide, 1.0 mM X-Gluc) for 30 min and incubated overnight in the dark at 37°C. Prior to observation, samples were cleared in a solution of ethanol and acetone (3:1) at room temperature for 15 h.

Sub-cellular localization

For sub-cellular localization, initially cNLS Mapper program was used to predict the nuclear localization signal (NLS) of *CabHLH10* protein sequence. The coding sequences of *Ca*bHLH10 was fused with C-terminal sequence of YFP (yellow fluorescent protein) by cloning into pSITE3CA vector under *CaMV* 35S promoter through gateway technology (Invitrogen, USA) according to the manufacturer's instructions using gene-specific primers (used for Y1H assay; Supplemental Table 14). The YFP fusion constructs along with empty vector (control) were transiently expressed in onion epidermal cells through particle bombardment-based transformation using a Biolistic^{R}-PDS-1000/He Particle Delivery System (Bio-Rad, USA) as described by Sharma et al. (2015). After 12–18 h incubation at 28°C, YFP fluorescence signals were observed under a Leica TCS SP8 confocal laser scanning microscope (Leica, Germany) using a 20x Dry objective lenses (HC PL APO 20x/0.75 CS2). YFP fluorescence was excited at 514 nm using an argon laser at 15% intensity and emission at 530 nm detected using a HyD1 detector with a gain of 68% and with a collection band width of 520–560 nm.

Plant growth conditions and treatments

The low and high DYI(P/H) NILs/ILs were grown in the pots-containing the agropeat:vermiculite (3:1) mixture at the plant growth chamber as described (Meena et al., 2015). Subsequently, 20-days-old seedlings were used for moisture and hormonal stress and root histological studies. The plants were subjected to dehydration/moisture stress by placing the seedlings on the folds of tissue paper for 12 h treatment at 22 ± 1°C (Garg et al., 2015; Deokar et al., 2015). For ABA treatment, the roots of aforesaid plants were dipped in 100 μM ABA (A1049, Sigma, USA) solution while the control plants were dipped in normal water for 12 h following Meena et al. (2015). The NILs/ILs were grown hydroponically in

Hoagland solutions and subjected to dehydration stress as per aforementioned methods. The seeds of NILs/ILs were also germinated on MS (Murashige and Skoog basal salt mixture)-phytagel medium for 10–15 days without (control) or with 100 µM ABA in a controlled environment to study the response of their roots and shoots towards ABA stress both at the germination and vegetative stage. Three biological replicates representing both control unstressed and dehydration/ABA stress-imposed roots and shoots of NILs/ILs were collected and stored at −80°C until RNA extraction for further study. The NILs/ILs were grown in the rainout shelter and phenotyped for diverse root and shoot agro-morphological traits under control unstressed and drought stress conditions (withheld water for 30 days after seedling establishment) as per RCBD with three replications using a cylinder culture method following Kashiwagi et al. (2005).

Vector construction and generation of transgenic plants

Full-length coding sequence (741 bp) of the *CabHLH10* was amplified from cDNA of a chickpea accession ICC 4958, obtained by RT-qPCR (Verso cDNA synthesis Kit, Thermo Scientific) using gene-specific primers (CabHLH10_pBI_Fand CabHLH10_pBI_R) enlisted in Supplemental Table 14. The amplicon was ligated at the *Xba*I and *BamH*I sites of the binary plant vector pBI121 (Clontech Laboratories, USA), under the control of *CaMV* 35S promoter. The resulting construct (*35S:CabHLH10*) was introduced into the *Agrobacterium tumefaciens* strain GV3101. The *in-planta Agrobacterium*-mediated transformation of chickpea Pusa 362 (*desi*) cotyledons/seeds was performed following previous protocols (Chakraborti et al., 2006; Das et al., 2021). The transformants were screened by PCR and RT-qPCR analysis for transgene detection and expression level, respectively. Transgenic lines with single copy transgene were detected by Southern blotting. The homozygous transgenic lines were grown till T_3 generation under green-house conditions and were assessed for its drought stress response.

For complementation study, seeds of the T-DNA insertion *Arabidopsis* mutants of *bHLH10* (SALK_046700) were obtained from the *Arabidopsis* Biological Resource Center (ABRC). The wild type (WT) used in this study was *Arabidopsis* ecotype Columbia-0. Transformation of the *Arabidopsis bHLH10* mutant using the aforementioned transformed *Agrobacterium* strain was carried out using the floral-dip method (Clough and Bent, 1998). Positive transformants were selected by plating the transformed seeds on ½ MS (Murashige and Skoog medium) supplemented with 50 mg/ml kanamycin (Kan) and further confirmed by PCR analysis using gene-specific primers. Chi-square (χ^2) test analysis based on segregation ratio of 3:1 was used to select transformants with single transgene copy number following Sharma et al. (2015). The homozygous transgenic lines were grown till T_2/T_3 generation and were assessed for its water-deficit stress response.

Phenotypic evaluation of transgenic chickpea and Arabidopsis

The WT (Pusa 362) and transgenic chickpea plants were assessed for their drought stress response using the soil cylinder culture (rainout shelter) following the aforesaid methods. Phenotypic evaluation of the WT, mutant, and transgenic *Arabidopsis* plants was performed to assess their water-deficit stress response. Seeds (50–100) were plated on solid MS medium with 1% sucrose and grown in growth chamber at 22 ± 1°C under continuous light (100 µmol $m^{-2}s^{-2}$). To evaluate the effect of ABA on root growth, 6-days-old WT, mutant, and transgenic seedlings were transferred to MS medium supplemented with ABA (0.5 and 1 µM). After 8–12 days of growth, the root length (cm), and lateral root number were measured using ImageJ 1.31 v software. To impose drought stress, 3-week-old soil-grown plants were subjected to water withholding for three weeks and recovery was given for 4 d. The RCW (relative water content), survival rate, and rate of water loss of the drought-stressed versus -unstressed control soil-grown plants were measured according to Sharma et al. (2015).

Phenotyping for PE traits

The control unstressed and drought/ABA stress-imposed low and high DYI(P/H) NILs were phenotyped for diverse PE trait parameters, including CC (mg/g-FW), SCMR, CF (Fv/Fm), CAR-CO_2↑ (µmol CO_2m^{-2} s^{-1}), and CAR-LI↑ (µmol CO_2m^{-2} s^{-1}) as per Basu et al. (2019). Three biological replicates each with at least three technical replicates were used for phenotyping of PE traits.

Accession numbers

The sequencing data have been submitted to the NCBI-sequence read archive (SRA) database (http://www.ncbi.nlm.nih.gov/sra) under accession number SRR6277501 (Submission ID: SUB3198514). All 110110 high-quality SNPs were submitted to NCBI dbSNP (http://www.ncbi.nlm.nih.gov/SNP/snp_viewTable.cgi?handle=NIPGR) (Supplemental Table 3) for unrestricted public access. Detailed information on all major genes/proteins mentioned in this manuscript can be found in the Supplemental Tables 3 and 8 and 12.

Supplemental data

The following materials are available in the online version of this article.

Supplemental Figure S1. Diagram illustrating the strategies followed to develop introgression lines (ILs) and their efficacy in genome-wide integrated genomics-assisted breeding to develop drought-tolerant chickpea cultivars with enhanced yield and productivity.

Supplemental Figure S2. Overview of plants and mature seeds of introgression lines (ILs) developed to dissect drought-tolerance traits in chickpea.

Supplemental Figure S3. A genome scan plot illustrating the overall genomic density and distribution of 110110 SNPs physically mapped across eight chromosomes of *kabuli* chickpea genome.

Supplemental Figure S4. Genomic distribution and structural annotation of 110110 genome-wide SNPs discovered from 222 ILs (association panel) along with six high-yielding cultivated (*desi* and *kabuli*) chickpea varieties and one wild progenitor *Cicer reticulatum* accession (used as parents to develop ILs) through GBS assay.

Supplemental Figure S5. Determination of molecular diversity and genetic structure patterns among 222 introgression lines (ILs) in the association panel of chickpea.

Supplemental Figure S6. Broad phenotypic variation of major seed yield traits observed among 222 ILs in a constituted association panel of chickpea during drought stress.

Supplemental Figure S7. Wide phenotypic variation of major seed yield traits observed among 222 ILs in a constituted association panel of chickpea during drought stress.

Supplemental Figure S8. GWAS-derived Manhattan plots generated using 48167 chromosome-wise SNPs, showing the significant *P* values of genomic SNP loci associated with major seed yield traits under drought stress in chickpea.

Supplemental Figure S9. Summary of GWAS-derived genomic SNP loci associated with major seed yield traits under drought stress in chickpea.

Supplemental Figure S10. Molecular mapping of major QTLs and eQTL governing vital seed yield traits during drought stress in chickpea.

Supplemental Figure S11. Marker (haplotype)-assisted selection led to development of drought-tolerant lines with enhanced yield and productivity in chickpea.

Supplemental Figure S12. Graphical genotypes of drought-tolerant lines developed through marker (haplotype)-assisted selection in chickpea.

Supplemental Figure S13. Genomic distribution and constitution of 129 *CabHLH* transcription factor (TF) genes scanned and annotated from *kabuli* chickpea genome.

Supplemental Figure S14. High-resolution molecular mapping identified major eQTLs [*CaeqDYI(P/H)1.1*] genomic region of *CaRD22*, *CaCAB* protein, and basic leucine zipper (*CabZIP*) governing yield traits under drought stress in chickpea.

Supplemental Figure S15. Controlled environment phenotyping exhibited enhanced root morphometric trait characteristics without compensating shoot growth/development in the drought-tolerant *CabHLH10* gene haplotype-introgressed lines during drought and ABA stress.

Supplemental Figure S16. Phenotypic evaluation of drought-tolerant lines developed through marker (haplotype)-assisted selection for yield and productivity traits under drought stress.

Supplemental Figure S17. Overexpression of *CabHLH10* improves root/shoot agro-morphological trait characteristics and enhanced drought tolerance in transgenic chickpea.

Supplemental Figure S18. Overexpression of *CabHLH10* in *Arabidopsis bHLH10* mutant enhances drought tolerance.

Supplemental Table S1. An association panel constituted comprising of 222 introgression lines (ILs) along with seven accessions (used as parents to develop ILs) utilized for genetic dissection of major yield traits during drought stress in chickpea.

Supplemental Table S2. Summary of sequencing statistics generated through GBS of 222 introgression lines (ILs) belonging to an association panel as well as seven accessions used as parents to develop ILs of chickpea.

Supplemental Table S3. Structural and functional annotation of 110110 genome-wide SNPs discovered through GBS of 222 introgression lines (ILs) belonging to an association panel along with seven accessions used as parents to develop ILs of chickpea.

Supplemental Table S4. Descriptive statistics of major yield traits measured among 222 introgression lines (ILs) in an association panel constituted based on their multi-environment replicated field phenotyping under irrigated (unstressed) and unirrigated (drought stress) conditions.

Supplemental Table S5. Genomic SNP loci significantly associated with major yield traits under drought stress in chickpea.

Supplemental Table S6. SNPs mapped on eight chromosomes of a high-density genetic linkage map of chickpea.

Supplemental Table S7. Genomic constitution based on structural and functional annotation of *CabHLH* genes identified from chickpea genome.

Supplemental Table S8. Summary of *CabHLH10* gene of chickpea exhibiting orthologous relationship with other legumes and *Arabidopsis*.

Supplemental Table S9. Germplasm accessions selected for molecular haplotyping to dissect major yield traits under drought stress in chickpea.

Supplemental Table S10. Wild *Cicer* accessions used for molecular haplotyping to dissect major yield traits under drought stress in chickpea.

Supplemental Table S11. Agro-morphological traits-based phenotyping depicting variation for major root and shoot morphometric traits in the 30-days-old cylinder-soil-grown plants of drought-tolerant and sensitive near isogenic lines (NILs).

Supplemental Table S12. ABA-responsive candidate/known genes controlling drought tolerance in crop plants assayed through global transcriptome sequencing used for differential expression profiling in the high- and low-DYI near isogenic lines (NILs) of chickpea.

Supplemental Table S13. Seed yield traits evaluated in the high- and low-DYI near isogenic lines (NILs) vis-à-vis high-yielding cultivated accessions (parents to develop ILs) of chickpea based on their multi-environment replicated field phenotyping under irrigated (unstressed) and unirrigated (drought stress) conditions.

Supplemental Table S14. Details of primers used in the present study for functional genomic analysis.

Acknowledgments

We are thankful to Mr. Sube Singh, lead scientific officer, Grain Legumes Research Program/Genebank, ICRISAT, Hyderabad for assisting in collecting multi-environment field phenotyping data for the introgression lines (ILs), germplasm accessions, and mapping population. We are very grateful to all of the scientific and technical staff members of NIPGR and IARI (Indian Council of Agricultural Research), New Delhi and ICRISAT, Hyderabad who provided valuable guidance, suggestions, constant encouragement, and timely support of the research. We are also thankful to the Central Instrumentation Facility (CIF), Plant Growth Facility (PGF), and DBT-eLibrary Consortium (DeLCON) of NIPGR, New Delhi for providing timely support and access to e-resources for this study.

Funding

Financial support for this study was provided by a research grant from the Department of Biotechnology (DBT), Ministry of Science and Technology, India (102/IFD/SAN/2161/2013-14). V.T., U.B., L.N., A.D., and J.K.M. acknowledge the UGC (University Grants Commission) and DBT, India for research fellowship awards.

Conflict of interest statement. The authors declare that they have no competing interests.

Data availability

The sequencing data have been submitted to the NCBI-sequence read archive (SRA) database (http://www.ncbi.nlm.nih.gov/sra) under accession number SRR6277501 (Submission ID: SUB3198514). All 110110 high-quality SNPs were submitted to NCBI dbSNP (http://www.ncbi.nlm.nih.gov/SNP/snp_viewTable.cgi?handle=NIPGR) (Supplemental Table 3) for unrestricted public access. Detailed information about all of the work described in this manuscript can be found in the Supplemental Data.

References

Abe H, Urao T, Ito T, Seki M, Shinozaki K, Yamaguchi-Shinozaki K (2003) *Arabidopsis AtMYC2* (*bHLH*) and *AtMYB2* (*MYB*) function as transcriptional activators in abscisic acid signaling. Plant Cell **15**(1): 63–78

Abe H, Yamaguchi-Shinozaki K, Urao T, Iwasaki T, Hosokawa D, Shinozaki K (1997) Role of *Arabidopsis MYC* and *MYB* homologs in drought- and abscisic acid-regulated gene expression. Plant Cell **9**(10): 1859–1868

Bajaj D, Saxena MS, Kujur A, Das S, Badoni S, Tripathi S, Upadhyaya HD, Gowda CL, Sharma S, Singh S, et al. (2015a) Genome-wide conserved non-coding microsatellite (CNMS) marker-based integrative genetical genomics for quantitative dissection of seed weight in chickpea. J Exp Bot **66**(5): 1271–1290

Bajaj D, Upadhyaya HD, Khan Y, Das S, Badoni S, Shree T, Kumar V, Tripathi S, Gowda CL, Singh S, et al. (2015b) A combinatorial approach of comprehensive QTL-based comparative genome mapping and transcript profiling identified a seed weight-regulating candidate gene in chickpea. Sci Rep **5**(1): 9264

Bao G, Zhuo C, Qian C, Xiao T, Guo Z, Lu S (2016) Co-expression of NCED and ALO improves vitamin C level and tolerance to drought and chilling in transgenic tobacco and stylo plants. Plant Biotechnol J **14**(1): 206–214

Basu U, Bajaj D, Sharma A, Malik N, Daware A, Narnoliya L, Thakro V, Upadhyaya HD, Kumar R, Tripathi S, et al. (2019) Genetic dissection of photosynthetic efficiency traits for enhancing seed yield in chickpea. Plant Cell Environ **42**(1): 158–173

Bharadwaj C, Tripathi S, Soren KR, Thudi M, Singh RK, Sheoran S, Roorkiwal M, Patil BS, Chitikineni A, Palakurthi R, et al. (2021) Introgression of "QTL-hotspot" region enhances drought tolerance and grain yield in three elite chickpea cultivars. Plant Genome **14**(1): e20076

Bradbury PJ, Zhang Z, Kroon DE, Casstevens TM, Ramdoss Y, Buckler ES (2007) TASSEL: software for association mapping of complex traits in diverse samples. Bioinformatics **23**(19): 2633–2635

Catchen J, Hohenlohe PA, Bassham S, Amores A, Cresko WA (2013) Stacks: an analysis tool set for population genomics. Mol Ecol **22**(11): 3124–3140

Chakraborti D, Sarkar A, Das S (2006) Efficient and rapid in vitro plant regeneration system for Indian cultivars of chickpea (*Cicer arietinum* L.). Plant Cell Tissue Organ Cult **86**(1): 117–123

Clough SJ, Bent AF (1998) Floral dip: a simplified method for *Agrobacterium*-mediated transformation of *Arabidopsis thaliana*. Plant J **16**(6): 735–743

Dar NA, Amin I, Wani W, Wani SA, Shikari AB, Wani SH, Masoodi KZ (2017) Abscisic acid: a key regulator of abiotic stress tolerance in plants. Plant Gene **11**(Pt B): 106–111

Das A, Basu PS, Kumar M, Ansari J, Shukla A, Thakur S, Singh P, Datta S, Chaturvedi SK, Sheshshayee MS, et al. (2021) Transgenic chickpea (*Cicer arietinum* L.) harbouring *AtDREB1a* are physiologically better adapted to water deficit. BMC Plant Biol **21**(1): 39

Das S, Upadhyaya HD, Srivastava R, Bajaj D, Gowda CL, Sharma S, Singh S, Tyagi AK, Parida SK (2015) Genome-wide insertion-deletion (InDel) marker discovery and genotyping for genomics-assisted breeding applications in chickpea. DNA Res **22**(5): 377–386

Dave A, Hernández ML, He Z, Andriotis VM, Vaistij FE, Larson TR, Graham IA (2011) 12-oxo-phytodienoic Acid accumulation during seed development represses seed germination in *Arabidopsis*. Plant Cell **23**(2): 583–599

Deokar AA, Kondawar V, Kohli D, Aslam M, Jain PK, Karuppayil SM, Varshney RK, Srinivasan R (2015) The *CarERF* genes in chickpea (*Cicer arietinum* L.) and the identification of CarERF116 as abiotic stress responsive transcription factor. Funct Integr Genomics **15**(1): 27–46

De Souza AP, Massenburg LN, Jaiswal D, Cheng S, Shekar R, Long SP (2017) Rooting for cassava: insights into photosynthesis and associated physiology as a route to improve yield potential. New Phytol **213**(1): 50–65

Dombrecht B, Xue GP, Sprague SJ, Kirkegaard JA, Ross JJ, Reid JB, Fitt GP, Sewelam N, Schenk PM, Manners JM, et al. (2007) *MYC2* Differentially modulates diverse jasmonate-dependent functions in *Arabidopsis*. Plant Cell **19**(7): 2225–2245

Dwivedi V, Parida SK, Chattopadhyay D (2017) A repeat length variation in myo-inositol monophosphatase gene contributes to seed size trait in chickpea. Sci Rep **7**(1): 4764

Elshire RJ, Glaubitz JC, Sun Q, Poland JA, Kawamoto K, Buckler ES, Mitchell SE (2011) A robust, simple genotyping-by-sequencing (GBS) approach for high diversity species. PLoS One **6**(5): e19379

Evanno G, Regnaut S, Goudet J (2005) Detecting the number of clusters of individuals using the software STRUCTURE: a simulation study. Mol Ecol **14**(8): 2611–2620

Fang X, Turner NC, Yan G, Li F, Siddique KH (2010) Flower numbers, pod production, pollen viability, and pistil function are reduced and flower and pod abortion increased in chickpea (*Cicer arietinum* L.) under terminal drought. J Exp Bot **61**(2): 335–345

Garg R, Bhattacharjee A, Jain M (2015) Genome-scale transcriptomic insights into molecular aspects of abiotic stress responses in chickpea. Plant Mol Biol Rep **33**(3): 388–400

Garg R, Sahoo A, Tyagi AK, Jain M (2010) Validation of internal control genes for quantitative gene expression studies in chickpea (*Cicer arietinum* L.). Biochem Biophys Res Commun **396**(2): 283–288

Gaur PM, Samineni S, Tripathi S, Varshney RK, Gowda CLL (2015) Allelic relationships of flowering time genes in chickpea. Euphytica **203**(2): 295–308

Guan YS, Serraj R, Liu SH, Xu JL, Ali J, Wang WS, Venus E, Zhu LH, Li ZK (2010) Simultaneously improving yield under drought stress and non-stress conditions: a case study of rice (*Oryza sativa* L.). J Exp Bot **61**(15): 4145–4156

Guóth A, Tari I, Gallé Á, Csiszár J, Pécsváradi A, Cseuz L, Erdei L (2009) Comparison of the drought stress responses of tolerant and sensitive wheat cultivars during grain filling: changes in flag leaf photosynthetic activity, ABA levels, and grain yield. J Plant Growth Regul **28**(2): 167–176

Hamwieh A, Imtiaz M, Malhotra RS (2013) Multi-environment QTL analyses for drought-related traits in a recombinant inbred population of chickpea (*Cicer arietinum* L.). Theor Appl Genet **126**(4): 1025–1038

Hardy OJ, Vekemans X (2002) SPAGedi: a versatile computer program to analyse spatial genetic structure at the individual or population levels. Mol Ecol Notes **2**(4): 618–620

Jefferson RA, Kavanagh TA, Bevan MW (1987) GUS Fusions: beta-glucuronidase as a sensitive and versatile gene fusion marker in higher plants. EMBO J **6**(13): 3901–3907

Joehanes R, Nelson JC (2008) QGene 4.0, an extensible Java QTL-analysis platform. Bioinformatics **24**(23): 2788–2789

Kadam NN, Yin X, Bindraban PS, Struik PC, Jagadish KS (2015) Does morphological and anatomical plasticity during the vegetative stage make wheat more tolerant of water deficit stress than rice? Plant Physiol **167**(4): 1389–1401

Kashiwagi J, Krishnamurthy L, Gaur PM, Upadhyaya HD, Varshney RK, Tobita S (2013) Traits of relevance to improve yield under terminal drought stress in chickpea (*Cicer arietinum* L.). Field Crops Res **145**: 88–95

Kashiwagi J, Krishnamurthy L, Ramamoorthy P, Upadhyaya HD, Gowda CLL, Ito O, Varshney RK (2015) Scope for improvement of yield under drought through the root traits in chickpea (*Cicer arietinum* L.). Field Crops Res **170**: 47–54

Kashiwagi J, Krishnamurthy L, Upadhyaya HD, Krishna H, Chandra S, Vadez V, Serraj R (2005) Genetic variability of drought-avoidance root traits in the mini-core germplasm collection of chickpea (*Cicer arietinum* L.). Euphytica **146**(3): 213–222

Kazan K, Manners JM (2013) *MYC2*: the master in action. Mol Plant **6**(3): 686–703

Khandal H, Gupta SK, Dwivedi V, Mandal D, Sharma NK, Vishwakarma NK, Pal L, Choudhary M, Francis A, Malakar P, et al. (2020) Root-specific expression of chickpea cytokinin oxidase/-dehydrogenase 6 leads to enhanced root growth, drought tolerance and yield without compromising nodulation. Plant Biotechnol J **18**-(11): 2225–2240

Krishnamurthy L, Kashiwagi J, Upadhyaya HD, Gowda CLL, Gaur PM, Singh S, Ramamoorthy P, Varshney RK (2013) Partition coefficient-a trait that contributes to drought tolerance in chickpea. Field Crops Res **149**: 354–365

Krzywinski M, Schein J, Birol I, Connors J, Gascoyne R, Horsman D, Jones SJ, Marra MA (2009) Circos: an information aesthetic for comparative genomics. Genome Res **19**(9): 1639–1645

Kujur A, Bajaj D, Saxena MS, Tripathi S, Upadhyaya HD, Gowda CL, Singh S, Jain M, Tyagi AK, Parida SK (2013) Functionally relevant microsatellite markers from chickpea transcription factor genes for efficient genotyping applications and trait association mapping. DNA Res **20**(4): 355–374

Kujur A, Bajaj D, Upadhyaya HD, Das S, Ranjan R, Shree T, Saxena MS, Badoni S, Kumar V, Tripathi S, et al. (2015a) A genome-wide SNP scan accelerates trait-regulatory genomic loci identification in chickpea. Sci Rep **5**(1): 11166

Kujur A, Bajaj D, Upadhyaya HD, Das S, Ranjan R, Shree T, Saxena MS, Badoni S, Kumar V, Tripathi S, et al. (2015c) Employing genome-wide SNP discovery and genotyping strategy to extrapolate the natural allelic diversity and domestication patterns in chickpea. Front Plant Sci **6**: 162

Kujur A, Upadhyaya HD, Shree T, Bajaj D, Das S, Saxena MS, Badoni S, Kumar V, Tripathi S, Gowda CL, et al. (2015b) Ultra-high density intra-specific genetic linkage maps accelerate identification of functionally relevant molecular tags governing important agronomic traits in chickpea. Sci Rep **5**(1): 9468

Kumar V, Singh A, Mithra SV, Krishnamurthy SL, Parida SK, Jain S, Tiwari KK, Kumar P, Rao AR, Sharma SK, et al. (2015) Genome-wide association mapping of salinity tolerance in rice (*Oryza sativa*). DNA Res **22**(2): 133–145

Kumar S, Stecher G, Tamura K (2016) MEGA7: molecular evolutionary genetics analysis version 7.0 for bigger datasets. Mol Biol Evol **33**(7): 1870–1874

Langmead B, Salzberg SL (2012) Fast gapped-read alignment with Bowtie 2. Nat Methods **9**(4): 357–359

Li Y, Zhang J, Zhang J, Hao L, Hua J, Duan L, Zhang M, Li Z (2013) Expression of an *Arabidopsis* molybdenum cofactor sulphurase gene in soybean enhances drought tolerance and increases yield under field conditions. Plant Biotechnol J **11**(6): 747–758

Lipka AE, Tian F, Wang Q, Peiffer J, Li M, Bradbury PJ, Gore MA, Buckler ES, Zhang Z (2012) GAPIT: genome association and prediction integrated tool. Bioinformatics **2**(18): 2397–2399

Liu K, Muse SV (2005) Powermarker: an integrated analysis environment for genetic marker analysis. Bioinformatics **21**(9): 2128–2129

Maccaferri M, Sanguineti MC, Corneti S, Ortega JL, Salem MB, Bort J, DeAmbrogio E, del Moral LF, Demontis A, El-Ahmed A, et al. (2008) Quantitative trait loci for grain yield and adaptation of durum wheat (*Triticum durum* Desf.) across a wide range of water availability. Genetics **178**(1): 489–511

Malik N, Dwivedi N, Singh AK, Parida SK, Agarwal P, Thakur JK, Tyagi AK (2016) An integrated genomic strategy delineates candidate mediator genes regulating grain size and weight in rice. Sci Rep **6**(1): 23253

Mannur DM, Babbar A, Thudi M, Sabbavarapu MM, Roorkiwal M, Yeri SB, Bansal VP, Jayalakshmi SK, Singh Yadav S, Rathore A, et al. (2019) Super Annigeri 1 and improved JG 74: two Fusarium wilt-resistant introgression lines developed using marker-assisted backcrossing approach in chickpea (*Cicer arietinum* L.). Mol Breed **39**(1): 2

Mao H, Jian C, Cheng X, Chen B, Mei F, Li F, Zhang Y, Li S, Du L, Li T, et al. (2022) The wheat ABA receptor gene TaPYL1-1B contributes to drought tolerance and grain yield by increasing water-use efficiency. Plant Biotechnol J **20**(5): 846–861

Meena MK, Ghawana S, Dwivedi V, Roy A, Chattopadhyay D (2015) Expression of chickpea CIPK25 enhances root growth and tolerance to dehydration and salt stress in transgenic tobacco. Front Plant Sci **6**: 683

Melo JO, Martins LGC, Barros BA, Pimenta MR, Lana UGP, Duarte CEM, Pastina MM, Guimaraes CT, Schaffert RE, Kochian LV, et al. (2019) Repeat variants for the *SbMATE* transporter protect sorghum roots from aluminum toxicity by transcriptional interplay in *cis* and *trans*. Proc Natl Acad Sci USA **116**(1): 313–318

Mir RR, Zaman-Allah M, Sreenivasulu N, Trethowan R, Varshney RK (2012) Integrated genomics, physiology and breeding approaches for improving drought tolerance in crops. Theor Appl Genet **125**(4): 625–645

Miyazaki J, Stiller WN, Truong TT, Xu Q (2014) Jasmonic acid is associated with resistance to twospotted spider mites in diploid cotton (*Gossypium arboreum*). Funct Plant Biol **41**(7): 748–757

Muhammad Aslam M, Waseem M, Jakada BH, Okal EJ, Lei Z, Saqib HSA, Yuan W, Xu W, Zhang Q (2022) Mechanisms of abscisic acid-mediated drought stress responses in plants. Int J Mol Sci **23**(3): 1084

Mukhopadhyay P, Tyagi AK (2015) *OsTCP19* influences developmental and abiotic stress signaling by modulating ABI4-mediated pathways. Sci Rep **5**(1): 9998

Nakashima K, Yamaguchi-Shinozaki K, Shinozaki K (2014) The transcriptional regulatory network in the drought response and its crosstalk in abiotic stress responses including drought, cold, and heat. Front Plant Sci **5**: 170

Nei M, Tajima F, Tateno Y (1983) Accuracy of estimated phylogenetic trees from molecular data. II. Gene frequency data. J Mol Evol **19**(2): 153–170

Oh SJ, Song SI, Kim YS, Jang HJ, Kim SY, Kim M, Kim YK, Nahm BH, Kim JK (2005) *Arabidopsis CBF3/DREB1A* and *ABF3* in transgenic rice increased tolerance to abiotic stress without stunting growth. Plant Physiol **138**(1): 341–351

Pang J, Turner NC, Khan T, Du YL, Xiong JL, Colmer TD, Devilla R, Stefanova K, Siddique KHM (2017) Response of chickpea (*Cicer arietinum* L.) to terminal drought: leaf stomatal conductance, pod abscisic acid concentration, and seed set. J Exp Bot **68**(8): 1973–1985

Patel RK, Jain M (2012) NGS QC toolkit: a toolkit for quality control of next generation sequencing data. PLoS One **7**(2): e30619

Peña-Valdivia CB, Sánchez-Urdaneta AB, Rangel JM, Muñoz JJ, García-Nava R, Velázquez RC (2010) Anatomical root variations in response to water deficit: wild and domesticated common bean (*Phaseolus vulgaris* L). Biol Res **43**(4): 417–427

Pratap A, Chaturvedi SK, Tomar R, Rajan N, Malviya N, Thudi M, Saabale PR, Prajapati U, Varshney RK, Singh NP (2017) Marker-assisted introgression of resistance to fusarium wilt race 2 in Pusa 256, an elite cultivar of desi chickpea. Mol Genet Genomics **292**(6): 1237–1245

Prince SJ, Murphy M, Mutava RN, Durnell LA, Valliyodan B, Shannon JG, Nguyen HT (2017) Root xylem plasticity to improve water use and yield in water-stressed soybean. J Exp Bot **68**(8): 2027–2036

Pritchard JK, Stephens M, Donnelly P (2000) Inference of population structure using multilocus genotype data. Genetics **155**(2): 945–959

Purcell S, Neale B, Todd-Brown K, Thomas L, Ferreira MA, Bender D, Maller J, Sklar P, de Bakker PI, Daly MJ, et al. (2007) PLINK: a tool set for whole-genome association and population-based linkage analyses. Am J Hum Genet **81**(3): 559–575

Ramamoorthy P, Lakshmanan K, Upadhyaya HD, Vadez V, Varshney RK (2016) Shoot traits and their relevance in terminal drought tolerance of chickpea (*Cicer arietinum* L.). Field Crops Res **197**: 10–27

Ramamoorthy P, Lakshmanan K, Upadhyaya HD, Vadez V, Varshney RK (2017) Root traits confer grain yield advantages under terminal drought in chickpea (*Cicer arietinum* L.). Field Crops Res **201**: 146–161

Ramamoorthy P, Zaman-Allah M, Mallikarjuna N, Pannirselvam R, Krishnamurthy L, Gowda CLL (2013) Root anatomical traits and their possible contribution to drought tolerance in grain legumes. Plant Prod Sci **16**(1): 1–8

Raman A, Verulkar S, Mandal N, Variar M, Shukla V, Dwivedi J, Singh B, Singh O, Swain P, Mall A, et al. (2012) Drought yield index to select high yielding rice lines under different drought stress severities. Rice **5**(1): 31

Ramírez V, Coego A, López A, Agorio A, Flors V, Vera P (2009) Drought tolerance in *Arabidopsis* is controlled by the *OCP3* disease resistance regulator. Plant J **58**(4): 929

Ranjan R, Khurana R, Malik N, Badoni S, Parida SK, Kapoor S, Tyagi AK (2017) *bHLH142* regulates various metabolic pathway-related genes to affect pollen development and anther dehiscence in rice. Sci Rep **7**(1): 43397

Roca Paixão JF, Gillet FX, Ribeiro TP, Bournaud C, Lourenço-Tessutti IT, Noriega DD, Melo BP, de Almeida-Engler J, Grossi-de-Sa MF (2019) Improved drought stress tolerance in *Arabidopsis* by CRISPR/dCas9 fusion with a histone acetyl transferase. Sci Rep **9**(1): 8080

Rockman MV, Kruglyak L (2009) Recombinational landscape and population genomics of *Caenorhabditis elegans*. PLoS Genet **5**(3): e1000419

Saengwilai P, Nord EA, Chimungu JG, Brown KM, Lynch JP (2014) Root cortical aerenchyma enhances nitrogen acquisition from low-nitrogen soils in maize. Plant Physiol **166**(2): 726–735

Sah SK, Reddy KR, Li J (2016) Abscisic acid and abiotic stress tolerance in crop plants. Front Plant Sci **7**: 571

Saxena MS, Bajaj D, Das S, Kujur A, Kumar V, Singh M, Bansal KC, Tyagi AK, Parida SK (2014a) An integrated genomic approach for rapid delineation of candidate genes regulating agro-morphological traits in chickpea. DNA Res **21**(6): 695–710

Saxena MS, Bajaj D, Kujur A, Das S, Badoni S, Kumar V, Singh M, Bansal KC, Tyagi AK, Parida SK (2014b) Natural allelic diversity, genetic structure and linkage disequilibrium pattern in wild chickpea. PLoS One **9**(9): e107484

Schindelin J, Rueden CT, Hiner MC, Eliceiri KW (2015) The ImageJ ecosystem: an open platform for biomedical image analysis. Mol Reprod Dev **82**(7–8): 518–529

Selvaraj MG, Ishizaki T, Valencia M, Ogawa S, Dedicova B, Ogata T, Yoshiwara K, Maruyama K, Kusano M, Saito K, et al. (2017) Overexpression of an *Arabidopsis thaliana* galactinol synthase gene improves drought tolerance in transgenic rice and increased grain yield in the field. Plant Biotechnol J **15**(11): 1465–1477

Sharma G, Giri J, Tyagi AK (2015) Rice *OsiSAP7* negatively regulates ABA stress signalling and imparts sensitivity to water-deficit stress in *Arabidopsis*. Plant Sci **237**: 80–92

Sheen J (2001) Signal transduction in maize and *Arabidopsis* mesophyll protoplasts. Plant Physiol **127**(4): 1466–1475

Shimray PW, Bajaj D, Srivastava R, Daware A, Upadhyaya HD, Kumar R, Bharadwaj C, Tyagi AK, Parida SK (2017) Identifying transcription factor genes associated with yield traits in chickpea. Plant Mol Biol Rep **35**(5): 562–574

Shinozaki KY, Shinozaki K (2006) Transcriptional regulatory networks in cellular responses and tolerance to dehydration and cold stresses. Annu Rev Plant Biol **57**(1): 781–803

Shinozaki K, Yamaguchi-Shinozaki K (2007) Gene networks involved in drought stress response and tolerance. J Exp Bot **58**(2): 221–227

Singh VK, Khan AW, Jaganathan D, Thudi M, Roorkiwal M, Takagi H, Garg V, Kumar V, Chitikineni A, Gaur PM, et al. (2016) QTL-seq for rapid identification of candidate genes for 100-seed weight and root/total plant dry weight ratio under rainfed conditions in chickpea. Plant Biotechnol J **14**(11): 2110–2119

Singh D, Laxmi A (2015) Transcriptional regulation of drought response: a tortuous network of transcriptional factors. Front Plant Sci **6**: 895

Sivamani E, Bahieldin1 A, Wraith JM, Al-Niemi T, Dyer WE, Ho TD, Qu R (2000) Improved biomass productivity and water use efficiency under water deficit conditions in transgenic wheat constitutively expressing the barley *HVA1* gene. Plant Sci **155**(1): 1–9

Spindel J, Wright M, Chen C, Cobb J, Gage J, Harrington S, Lorieux M, Ahmadi N, McCouch S (2013) Bridging the genotyping gap: using genotyping by sequencing (GBS) to add high-density SNP markers and new value to traditional bi-parental mapping and breeding populations. Theor Appl Genet **126**(11): 2699–2716

Srivastava R, Bajaj D, Malik A, Singh M, Parida SK (2016) Transcriptome landscape of perennial wild *Cicer microphyllum* uncovers functionally relevant molecular tags regulating agronomic traits in chickpea. Sci Rep **6**(1): 33616

Srivastava R, Upadhyaya HD, Kumar R, Daware A, Basu U, Shimray PW, Tripathi S, Bharadwaj C, Tyagi AK, Parida SK (2017) A multiple QTL-Seq strategy delineates potential genomic loci governing flowering time in chickpea. Front Plant Sci **8**: 1105

Sun T, Zhang Y, Li Y, Zhang Q, Ding Y, Zhang Y (2015) ChIP-seq reveals broad roles of *SARD1* and *CBP60g* in regulating plant immunity. Nat Commun **6**(1): 10159

Talebi R, Karami E (2011) Morphological and physiological traits associated with seed yield in different chickpea (Cicer arietinum L.) genotypes under irrigated and water-deficit environments. South Asian J Exp Biol **1**(6): 260–267

Tian X, Li X, Zhou W, Ren Y, Wang Z, Liu Z, Tang J, Tong H, Fang J, Bu Q (2017) Transcription factor *OsWRKY53* positively regulates

brassinosteroid signaling and plant architecture. Plant Physiol **175**(3): 1337–1349

Toledo-ortiz G, Huq E, Quail PH (2003) The *Arabidopsis* basic/Helix-loop-Helix transcription factor family. Plant Cell **15**(8): 1749–1770

Travaglia C, Cohen AC, Reinoso H, Castillo C, Bottini R (2007) Exogenous abscisic acid increases carbohydrate accumulation and redistribution to the grains in wheat grown under field conditions of soil water restriction. J Plant Growth Regul **26**(3): 285–289

Travaglia C, Herminda R, Rubén B (2009) Application of abscisic acid promotes yield in field-cultured soybean by enhancing production of carbohydrates and their allocation in seed. Crop Pasture Sci **6**(12): 1131–1136

Travaglia C, Reinoso H, Cohen A, Luna C, Tommasino E, Castillo C, Bottini R (2010) Exogenous ABA increases yield in field-grown wheat with moderate water restriction. J Plant Growth Regul **29**(3): 366–374

Tsujimoto H (2001) Production of near-isogenic lines and marked monosomic lines in common wheat (*Triticum aestivum*) cv. Chinese Spring. J Hered **92**(3): 254–259

Tuteja N (2007) Abscisic acid and abiotic stress signaling. Plant Signal Behav **2**(3): 135–138

Uga Y, Sugimoto K, Ogawa S, Rane J, Ishitani M, Hara N, Kitomi Y, Inukai Y, Ono K, Kanno N, et al. (2013) Control of root system architecture by DEEPER ROOTING 1 increases rice yield under drought conditions. Nat Gen **45**(9): 1097–1102

Umezawa T, Nakashima K, Miyakawa T, Kuromori T, Tanokura M, Shinozaki K, Yamaguchi-Shinozaki K (2010) Molecular basis of the core regulatory network in ABA responses: sensing, signaling and transport. Plant Cell Physiol **51**(11): 1821–1839

Upadhyaya HD, Bajaj D, Das S, Saxena MS, Badoni S, Kumar V, Tripathi S, Gowda CL, Sharma S, Tyagi AK, et al. (2015) A genome-scale integrated approach aids in genetic dissection of complex flowering time trait in chickpea. Plant Mol Biol **89**(4–5): 403–420

Upadhyaya HD, Kashiwagi J, Varshney RK, Gaur PM, Saxena KB, Krishnamurthy L, Gowda CL, Pundir RP, Chaturvedi SK, Basu PS, et al. (2012) Phenotyping chickpeas and pigeonpeas for adaptation to drought. Front Physiol **3**: 179

Van Ooijen JW (2009) MapQTL 6: Software for the mapping of quantitative trait loci in experimental populations of diploid species. Kyazma BV, Wageningen, Netherlands

Varshney RK, Gaur PM, Siva K, Krishnamurthy CL, Tripathi S, Kashiwagi J, Samineni S, Singh VK, Thudi M, Jaganathan D (2013b) Fast-Track introgression of "QTL-hotspot" for root traits and other drought tolerance traits in JG 11, an elite and leading variety of chickpea. Plant Genome **6**(3): 3

Varshney RK, Mohan SM, Gaur PM, Chamarthi SK, Singh VK, Srinivasan N, Swapna N, Sharma M, Singh S, Kaur L, et al. (2014b) Marker-assisted backcrossing to introgress resistance to Fusarium wilt race 1 and Ascochyta blight in C 214, an elite cultivar of chickpea. Plant Genome **7**(1): 1

Varshney RK, Singh VK, Kumar A, Powell W, Sorrells ME (2018b) Can genomics deliver climate-change ready crops? Curr Opin Plant Biol **45**(Pt B): 205–211

Varshney RK, Song C, Saxena RK, Azam S, Yu S, Sharpe AG, Cannon S, Baek J, Rosen BD, Tar'an B, et al. (2013a) Draft genome sequence of chickpea (*Cicer arietinum*) provides a resource for trait improvement. Nat Biotechnol **31**(3): 240–246

Varshney RK, Thudi M, Nayak SN, Gaur PM, Kashiwagi J, Krishnamurthy L, Jaganathan D, Koppolu J, Bohra A, Tripathi S, et al. (2014a) Genetic dissection of drought tolerance in chickpea (*Cicer arietinum* L.). Theor Appl Genet **127**(2): 445–462

Varshney RK, Tuberosa R, Tardieu F (2018a) Progress in understanding drought tolerance: from alleles to cropping systems. J Exp Bot **69**-(13): 3175–3179

Venuprasad R, Impa SM, Gowda VRP, Atlin GN, Serraj R (2011) Rice near-isogenic-lines (NILs) contrasting for grain yield under lowland drought stress. Field Crops Res **123**(1): 38–46

Venuprasad R, Lafitte HR, Atlin GN (2007) Response to direct selection for grain yield under drought stress in rice. Crop Sci **47**(1): 285–293

Venuprasad R, Sta Cruz MT, Amante M, Magbanua R, Kumar A, Atlin GN (2008) Response to two cycles of divergent selection for grain yield under drought stress in four rice breeding populations. Field Crops Res **107**(3): 232–244

Voorrips RE (2002) Mapchart: software for the graphical presentation of linkage maps and QTLs. J Hered **93**(1): 77–78

Wang Y, Ying J, Kuzma M, Chalifoux M, Sample A, McArthur C, Uchacz T, Sarvas C, Wan J, Dennis DT, et al. (2005) Molecular tailoring of farnesylation for plant drought tolerance and yield protection. Plant J **43**(3): 413–424

Xiong L, Zhu JK (2003) Regulation of abscisic acid biosynthesis. Plant Physiol **133**(1): 29–36

Xu YH, Liu R, Yan L, Liu ZQ, Jiang SC, Shen YY, Wang XF, Zhang DP (2012) Light-harvesting chlorophyll a/b-binding proteins are required for stomatal response to abscisic acid in *Arabidopsis*. J Exp Bot **63**(3): 1095–1106

Yamori W, Kondo E, Sugiura D, Terashima I, Suzuki Y, Makino A (2016) Enhanced leaf photosynthesis as a target to increase grain yield: insights from transgenic rice lines with variable rieske FeS protein content in the cytochrome b6/f complex. Plant Cell Environ **39**(1): 80–87

Yang J, Zhang J, Wang Z, Zhu Q, Wang W (2001) Hormonal changes in the grains of rice subjected to water stress during grain filling. Plant Physiol **127**(1): 315–323

Yang J, Zhang J, Ye Y, Wang Z, Zhu Q, Liu L (2004) Involvement of abscisic acid and ethylene in the responses of rice grains to water stress during filling. Plant Cell Env **27**(8): 1055–1064

Yano K, Yamamoto E, Aya K, Takeuchi H, Lo PC, Hu L, Yamasaki M, Yoshida S, Kitano H, Hirano K (2016) Genome-wide association study using whole-genome sequencing rapidly identifies new genes influencing agronomic traits in rice. Nat Genet **48**(8): 927–934

Zhang Z, Ersoz E, Lai CQ, Todhunter RJ, Tiwari HK, Gore MA, Bradbury PJ, Yu J, Arnett DK, Ordovas JM, et al. (2010) Mixed linear model approach adapted for genome-wide association studies. Nat Genet **42**(4): 355–360

Zhang W, Li A, Tian J, Zhao L (2012) Development of near isogenic lines of wheat carrying different spike branching genes and their agronomic and spike characters. J Agric Sci **4**(8): 215

Zhang L, Ming R, Zhang J, Tao A, Fang P, Qi J (2015) De novo transcriptome sequence and identification of major bast-related genes involved in cellulose biosynthesis in jute (*Corchorus capsularis* L.). BMC Genomics **16**(1): 1062

Zhang X, Wollenweber B, Jiang D, Liu F, Zhao J (2008) Water deficits and heat shock effects on photosynthesis of a transgenic *Arabidopsis thaliana* constitutively expressing *ABP9*, a *bZIP* transcription factor. J Exp Bot **59**(4): 839–848

Zhao K, Tung CW, Eizenga GC, Wright MH, Ali ML, Price AH, Norton GJ, Islam MR, Reynolds A, Mezey J, et al. (2011) Genome-wide association mapping reveals a rich genetic architecture of complex traits in *Oryza sativa*. Nat Commun **2**(1): 467

Zhao J, Zheng L, Wei J, Wang Y, Chen J, Zhou Y, Chen M, Wang F, Ma Y, Xu Z-S (2022) The soybean *PLATZ* transcription factor *GmPLATZ17* suppresses drought tolerance by interfering with stress-associated gene regulation of *GmDREB5*. Crop J **10**(4): 1014–1025

Zhu J, Brown KM, Lynch JP (2010) Root cortical aerenchyma improves the drought tolerance of maize (*Zea mays* L.). Plant Cell Environ **33**(5): 740–749

Zong W, Tang N, Yang J, Peng L, Ma S, Xu Y, Li G, Xiong L (2016) Feedback regulation of ABA signaling and biosynthesis by a *bZIP* transcription factor targets drought-resistance-related genes. Plant Physiol **171**(4): 2810–2825